

การเสริมแรงทางธรรมชาติด้วยแบคทีเรียเซลลูโลสโดยกระบวนการสารละลายลาเท็กซ์

นางสาวศิริลักษณ์ พรหมรักษ์

จุฬาลงกรณ์มหาวิทยาลัย
CHULALONGKORN UNIVERSITY

บทคัดย่อและแฟ้มข้อมูลฉบับเต็มของวิทยานิพนธ์ตั้งแต่ปีการศึกษา 2554 ที่ให้บริการในคลังปัญญาจุฬาฯ (CUIR)
เป็นแฟ้มข้อมูลของนิสิตเจ้าของวิทยานิพนธ์ ที่ส่งผ่านทางบัณฑิตวิทยาลัย

The abstract and full text of theses from the academic year 2011 in Chulalongkorn University Intellectual Repository (CUIR)
are the thesis authors' files submitted through the University Graduate School.

วิทยานิพนธ์นี้เป็นส่วนหนึ่งของการศึกษาตามหลักสูตรปริญญาวิศวกรรมศาสตรมหาบัณฑิต

สาขาวิชาวิศวกรรมเคมี ภาควิชาวิศวกรรมเคมี

คณะวิศวกรรมศาสตร์ จุฬาลงกรณ์มหาวิทยาลัย

ปีการศึกษา 2559

ลิขสิทธิ์ของจุฬาลงกรณ์มหาวิทยาลัย

REINFORCING NATURAL RUBBER WITH BACTERIAL CELLULOSE
VIA LATEX SOLUTION PROCESS

Miss Sirilak Phomrak



A Thesis Submitted in Partial Fulfillment of the Requirements
for the Degree of Master of Engineering Program in Chemical Engineering

Department of Chemical Engineering

Faculty of Engineering

Chulalongkorn University

Academic Year 2016

Copyright of Chulalongkorn University

Thesis Title REINFORCING NATURAL RUBBER WITH BACTERIAL
CELLULOSE VIA LATEX SOLUTION PROCESS

By Miss Sirilak Phomrak

Field of Study Chemical Engineering

Thesis Advisor Associate Professor Muenduen Phisalaphong,
Ph.D.

Accepted by the Faculty of Engineering, Chulalongkorn University in Partial
Fulfillment of the Requirements for the Master's Degree

.....Dean of the Faculty of Engineering
(Associate Professor Supot Teachavorasinskun, D.Eng.)

THESIS COMMITTEE

.....Chairman
(Associate Professor Seeroong Prichanont, Ph.D.)

.....Thesis Advisor
(Associate Professor Muenduen Phisalaphong, Ph.D.)

.....Examiner
(Professor Artiwan Shotipruk, Ph.D.)

.....External Examiner
(Sirijutaratana Covavisaruch, Ph.D.)

ศิริลักษณ์ พรหมรักษ์ : การเสริมแรงยางธรรมชาติด้วยแบคทีเรียเซลลูโลสโดยกระบวนการ
สารละลายลาเท็กซ์ (REINFORCING NATURAL RUBBER WITH BACTERIAL
CELLULOSE VIA LATEX SOLUTION PROCESS) อ.ที่ปรึกษาวิทยานิพนธ์หลัก: รศ. ดร.
เหมือนเดือน พิศาลพงศ์, 90 หน้า.

สมบัติความยืดหยุ่นที่โดดเด่นจึงทำให้ยางธรรมชาติเป็นวัสดุที่มีความสำคัญอย่างยิ่งใน
อุตสาหกรรมอิลาสโตเมอร์ เช่น ยางรถยนต์ ชิ้นส่วนภายในรถยนต์ ถุงมือ และบรรจุภัณฑ์ เป็นต้น แต่
อย่างไรก็ตามยางธรรมชาติยังมีข้อด้อย ได้แก่ สมบัติการทนต่อแรงดึงและการทนต่อการขีดถูต่ำ
นอกจากนี้ การใช้ประโยชน์จากยางธรรมชาติยังถูกจำกัดด้วยสมบัติการทนต่อน้ำมันและสารที่มีสมบัติ
เป็นตัวทำละลายต่ำ หลายปีที่ผ่านมาการเตรียมคอมโพสิตของยางธรรมชาติที่เสริมแรงด้วยเซลลูโลส
ได้รับความสนใจเป็นอย่างมากเนื่องจากเป็นวิธีที่สามารถเพิ่มค่ายังโมดูลัสและการทนต่อแรงดึงของ
ยางธรรมชาติซึ่งเป็นการลดข้อด้อยและข้อจำกัดดังกล่าวข้างต้น ปกติในการเตรียมคอมโพสิตมักจะ
เกิดปัญหาการตกตะกอนและการกระจายตัวต่ำของเซลลูโลสภายในเนื้อยางธรรมชาติในขั้นตอนการ
ผสมซึ่งเป็นผลมาจากความแตกต่างของสภาพชั่วคราวของโมเลกุลยางธรรมชาติกับเซลลูโลส งานวิจัยนี้
จึงมีความมุ่งหวังที่จะพัฒนาสมบัติของยางธรรมชาติโดยการเสริมแรงด้วยแบคทีเรียเซลลูโลสซึ่งเป็น
วัสดุที่มีสมบัติหลายประการ ได้แก่ ความสามารถเข้ากันได้ดีกับร่างกาย ความสามารถในการ
เสริมแรง รวมไปถึงความชอบน้ำ ผ่านกระบวนการสารละลายลาเท็กซ์เพียงหนึ่งขั้นตอน และงานวิจัย
นี้ถูกขยายขอบเขตด้วยการเพิ่มเสถียรภาพทางโครงสร้างของคอมโพสิตผ่านกระบวนการการดัดแปลง
คอมโพสิตด้วยกรดอินทรีย์ ทั้งนี้ พิล์มคอมโพสิตและฟิล์มคอมโพสิตที่ผ่านการดัดแปลงด้วยกรดถูก
นำมาวิเคราะห์ทั้งทางด้านกายภาพ เคมี และชีวภาพ พบว่า การเตรียมคอมโพสิตยางธรรมชาติสำเร็จ
ลุล่วงตามวัตถุประสงค์โดยเส้นใยแบคทีเรียเซลลูโลสกระจายตัวอย่างสม่ำเสมอภายในเนื้อยาง
ธรรมชาติในทุกๆ ความเข้มข้น สมบัติเชิงกลของยางธรรมชาติถูกปรับปรุงโดยการเสริมแรงด้วย
แบคทีเรียเซลลูโลส ในขณะที่เสถียรภาพทางโครงสร้างของคอมโพสิตเพิ่มมากขึ้นหลังการดัดแปลง
ด้วยกรดอินทรีย์ อันตรกิริยาระหว่างยางธรรมชาติกับแบคทีเรียเซลลูโลสที่ผ่านการปรับปรุงไม่มี
ผลกระทบอย่างมีนัยสำคัญต่อความสามารถในการย่อยสลายของคอมโพสิตในดิน

ภาควิชา วิศวกรรมเคมี

ลายมือชื่อนิสิต

สาขาวิชา วิศวกรรมเคมี

ลายมือชื่อ อ.ที่ปรึกษาหลัก

ปีการศึกษา 2559

5670400821 : MAJOR CHEMICAL ENGINEERING

KEYWORDS: NATURAL RUBBER / BACTERIAL CELLULOSE / NANOCOMPOSITES

SIRILAK PHOMRAK: REINFORCING NATURAL RUBBER WITH BACTERIAL CELLULOSE VIA LATEX SOLUTION PROCESS. ADVISOR: ASSOC. PROF. MUENDUEN PHISALAPHONG, Ph.D., 90 pp.

Natural rubber (NR) is an important material for a variety of the elastomer industry such as tires, automotive interior parts, gloves as well as packaging due to the excellent elastic properties. However, there are some drawbacks such as low tensile strength and low abrasion resistance. Moreover, its applications are also limited because of its poor resistance to oil and solvents. Preparation of NR-composites reinforced with cellulose to enhance Young's modulus and tensile strength of the NR which is a decreasing solution to these defects and limitations has attracted much interest in recent years. Usually, in the mixing step of rubber-cellulose composite preparation, there are problems of agglomeration and low dispersion of cellulose due to the difference of molecular polarity between cellulose and NR. In this study, in order to enhance the properties of NR-composite films, we focus on NR reinforced with bacterial cellulose (BC) which has many advantages including biocompatibility, remarkable mechanical properties, and high hydrophilicity via one-step latex solution processing. In addition, this study will also explore the modification of NR-BC composites with organic acid to enhance the composite structural stability. The NR-BC composites (NRBC) and the acid modified NR-BC composites (ANRBC) films were characterized for physical, chemical and biological properties. The NRBC composites were successfully prepared via latex solution process. BC fibers dispersed homogeneously within the NR matrix for every concentration with different BC fiber contents. The mechanical properties of the NR-composite films were improved with the BC loading while the structural stability of ANRBC composites was enhanced after the acid modification. However, this improved NR-BC interaction had no significant effect on the biodegradability in soil.

Department: Chemical Engineering Student's Signature

Field of Study: Chemical Engineering Advisor's Signature

Academic Year: 2016

ACKNOWLEDGEMENTS

I would like to express my deepest gratitude to Associate Professor Dr. Muenduen Phisalaphong, my advisor, for her valuable advices and kind encouragement throughout this research work.

This project would have been impossible without the financial support of Ratchadaphiseksomphot Endowment Fund of Chulalongkorn University.

I am sincerely thankful to Associate Professor Dr. Seeroong Prichanont, the thesis committee chairman, Professor Dr. Artiwan Shotipruk and Dr. Sirijutaratana Covavisaruch, the thesis committee member, for their useful critiques of this research work and helpful suggestions.

I would like to thank Mr. Pairoj Anantasethakul, the staff from department of industrial engineering, and Mr. Bancha Ounpanich, the staff from Department of Nuclear Technology of Chulalongkorn University, for their constructive suggestion of biodegradability tests.

I would like to thank the Meteorological Department (Statue of Admiral Kromluang Chumporn Khate Udomsakdi in front of Headquarters, Bangkok, Thailand) for the daily weather reports.

A special thanks to comments, kindness and friendship from all student members of Associate Professor Muenduen groups as well as my friends in the lab of Chemical Engineering Research Unit for Value Adding of Bioresources.

Finally, I would like to thank my parents and my family members for their enthusiastic encouragement.

CONTENTS

	Page
THAI ABSTRACT	iv
ENGLISH ABSTRACT	v
ACKNOWLEDGEMENTS	vi
CONTENTS	vii
LIST OF FIGURES	x
LIST OF TABLES	xii
LIST OF ABBREVIATIONS	xiii
CHAPTER I INTRODUCTION.....	15
1.1 General introduction.....	15
1.2 The objectives of this research	17
1.3 The scope of this research.....	17
CHAPTER II BACKGROUND AND LITERATURE REVIEW.....	19
2.1 Natural rubber.....	19
2.2 Bacterial cellulose.....	20
2.3 Lactic acid.....	21
2.4 Polymer reinforcement.....	22
2.4.1 Composite preparation.....	22
2.4.2 Development of blending process.....	24
2.5 Cross-linked NR.....	30
CHAPTER III EXPERIMENTAL.....	32
3.1 Materials.....	32
3.2 Bacterial cellulose preparation	32

	Page
3.3 Preparation of NRBC composites	32
3.4 Modification of NRBC composites films via crosslinking process with organic acid	33
3.5 Characterization of the BC slurry	33
3.6 Characterization of the NR, BC, NRBC and ANRBC films.....	33
CHAPTER IV RESULTS AND DISCUSSION	38
4.1 Characterization of the BC slurry	38
4.1.1 Scanning electron microscopy (SEM).....	38
4.1.2 Particle size analysis with dynamic light scattering (DLS).....	38
4.2 Characterization of the NR, BC, NRBC and ANRBC films.....	39
4.2.1 Scanning electron microscopy (SEM).....	39
4.2.2 Fourier transform infrared (FTIR) spectroscopy	42
4.2.3 The transparency and opacity testing.....	43
4.2.4 The dynamic advancing and receding water contact angle analysis...44	
4.2.5 X-ray diffraction (XRD) analysis	46
4.2.6 Thermogravimetric analysis (TGA)	48
4.2.7 Differential scanning calorimetry (DSC)	51
4.2.8 Dynamical mechanical thermal analysis (DMTA)	53
4.2.9 Tensile testing.....	55
4.2.10 The solvent uptake study.....	58
4.2.11. The water vapor transmission rate (WVTR)	61
4.2.12 Biodegradation in soil	62
4.2.13 Anti-microbial ability	66

	Page
CHAPTER V CONCLUSIONS.....	68
REFERENCES	69
VITA.....	90



LIST OF FIGURES

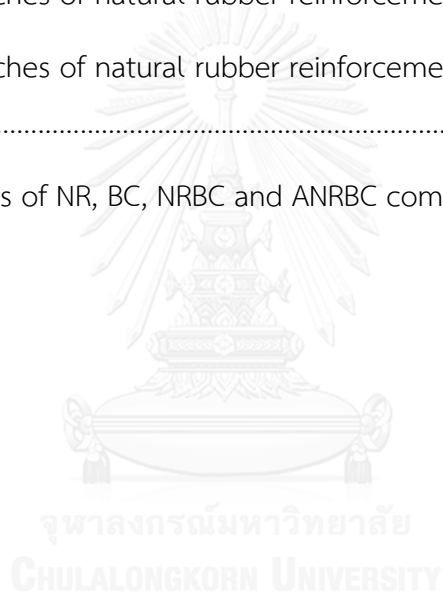
Figure	Page
Figure 2.1 Chemical structure of cis-1,4-polyisoprene.....	20
Figure 2.2 Chemical structure of BC	21
Figure 2.3 Chemical structure of lactic acid.....	21
Figure 4.1 SEM image of BC in the slurry.....	38
Figure 4.2 Particle size distribution of BC fiber.....	39
Figure 4.3 On the left, SEM images of the films of NR (A) and BC (B); on the right, enlarged view of the cross section of NR (C) and BC (D)	40
Figure 4.4 SEM images of the cross section of NRBC20(A), NRBC50(B), NRBC80(C), ANRBC20(D), ANRBC50(E), and ANRBC80(F)	41
Figure 4.5 FTIR spectra of NR, BC, NRBC and ANRBC composites	43
Figure 4.6 The opacity of NR, BC, NRBC, and ANRBC films	44
Figure 4.7 Dynamic water contact angle of NR, BC, NRBC and ANRBC composites.....	45
Figure 4.8 The interaction formation of the acid modification with lactic acid	46
Figure 4.9 XRD patterns of NR, BC, NRBC and ANRBC composites.....	47
Figure 4.10 Degree of crystallinity of NR, BC, NRBC and ANRBC composites.....	48
Figure 4.11 The TGA(A) and DTG(B) plot of NR, BC, NRBC, and ANRBC composites.....	50
Figure 4.12 The DSC chromatograms of NR, BC, NRBC, and ANRBC composites ...	52
Figure 4.13 The temperature dependence of the storage modulus (A) and $\tan \delta$ (B) of NR, BC, NRBC and ANRBC composites.....	54

Figure 4.14 Mechanical test data of NR, BC, NRBC and ANRBC composites	57
Figure 4. 15 The stress-strain curve of NR, BC, NRBC and ANRBC composites	58
Figure 4.16 Degree of swelling of NR, BC, NRBC and ANRBC composites in toluene (A) and water (B)	60
Figure 4.17 WVTR of NR, BC, NRBC and ANRBC composites.....	62
Figure 4.18 Biodegradation in soil of NR, BC, NRBC and ANRBC composites for 1(A), 3(B), and 6(C) months	65
Figure 4.19 Antibacterial ability of NR, BC, NRBC and ANRBC composites	67



LIST OF TABLES

Table	Page
Table 2.1 Components of fresh NRL	19
Table 2.2 The researches of natural rubber reinforcement via melt blending.....	26
Table 2.3 The researches of natural rubber reinforcement via melt blending (Continue).....	27
Table 2.4 The researches of natural rubber reinforcement via solution blending	28
Table 2.5 The researches of natural rubber reinforcement via solution blending (Continue).....	29
Table 4. 1 Weight loss of NR, BC, NRBC and ANRBC composites in soil.....	64



LIST OF ABBREVIATIONS

ANRBC	Acid modified natural rubber – bacterial cellulose composites
BC	Bacterial cellulose
BCPS	Bacterial cellulose coated with polystyrene
CNT	Carbon nanotubes
CNWS	Cellulose nanowhiskers
DCP	Dicumylperoxide
DI	Deionized
DLS	Dynamic light scattering
DMTA	Dynamical mechanical thermal analysis
DRC	Dry rubber content
DSC	Differential scanning calorimetry
FTIR	Fourier transform infrared
GO	Grapheme oxide
JFs	Short jute fiber
NR	Natural rubber
NRBC	Natural rubber – bacterial cellulose composites
NRBCPS	Natural rubber – bacterial cellulose coated with polystyrene composites
OMMT	Organically modified montmorillonite
Phr	Parts per hundred of rubber
SEM	Scanning electron microscopy
TEOS	Tetraethoxysilane

T_c	Crystallization temperature
T_g	Glass transition temperature
TGA	Thermogravimetric analysis
T_m	Melt temperature
VNRBC	Vulcanized - natural rubber – bacterial cellulose composites
VNRBCPS	Vulcanized - natural rubber – bacterial cellulose coated with polystyrene composites
WVTR	Water vapor transmission rate
XRD	X-ray diffraction



CHAPTER I

INTRODUCTION

1.1 General introduction

Thailand is the world's largest NR producer and exporter. NR is a processed plant product produced in various regions of Thailand. However, the price of natural rubber is unstable. Allowing the expansion of cultivated area, the NR price continuously declines due to the oversupply in the world market. In order to add more value and expand commercial utilization of NR, researches and development of NR-based products are required.

NR is a flexible polymer that has the ability to regain its original shape after being deformed and therefore, NR is used as a raw material in elastomer industry, including automotive and truck tires, the major NR market [1]. Nonetheless, some inferior properties of NR, such as low mechanical strength and abrasion resistance as well as poor resistance to oil and solvents can cause the disadvantages of the NR products. Moreover, its mechanical properties vary with temperature. Softness of NR increases with increasing temperature, while brittleness increases at lower temperature. Thus the structural modification is required to improve NR properties [2]. The reinforcement is the basic modification of the polymer properties thanks to it is easy to prepare. The reinforcement of NR considerably depends on reinforcing agents. In the past, nanoscopic additives such as carbon black and silica nanoparticle were main reagents for polymer reinforcement [3, 4]. Silica-reinforced NR prepared via the sol-gel process is one of the reinforcing methods that have been widely used [5-7]. Research studies for reinforcing additives are incessantly conducted, for instance, glass fiber, aramide, nylon, grapheme, sago starch, clay, carbon nanotubes and lignocellulosic fiber; wood flour, oil palm flour, cotton fiber as well as microcrystalline cellulose [8-15]. Focusing on green material development, NR and cellulose represent major biopolymers and renewable materials of high availability in Southeast Asia. Currently, nanocellulose produced by the bacteria *Acetobacter xylinum*, namely BC

has been studied for the use in both natural and synthetic polymer reinforcing [16-20]. However, without pretreatment, only low concentration of cellulose can be added in NR matrix because of the difference of the polarity between NR and cellulose. Effective methods for reducing this problem have been concerned. It has been reported that the preparation of NR composites via solution system instead of rubber melt blending could decrease the hydrophilicity and polarity of the nanofibers, and hence increase their adhesion to the rubber matrix [21].

Crosslinking process has also received much attention as a method for improving properties of rubber. The network structure formed under crosslinking conditions is the key leading to modified properties. One of the earliest examples of the crosslinking process is the vulcanization of rubber by adding sulfur under high temperature, which creates the links between the latex molecules. Vulcanization gives the rubber its strength over the temperature ranges in which non-vulcanized rubber could not perform. Furthermore, the cross links increases the toughness, strength and hardness of rubber. In particular, cross-linked rubber is resistant to attack of oxidizing agents [22]. Because of the side-effects of sulfur such as undesirable colors and toxicity, each organic acid was also used as cross-linking agents. Formic, maleic, stearic, citric as well as dicarboxylic acid are promoted acceleration of crosslinking in NR [23-27].

For this work, focusing on the preparation of NRBC composite films via solution method by adding slurry of BC into NRL as reinforcing fibers for the NR composite films. This study will also explore the modification of NRBC composites with organic acid to improve the performance of composite films. The characteristics of the films with the difference condition produced by both approaches would be evaluated and compared. Ultimately, the main objective of this work is to develop NR composite films, which can be further applied in the fields of packaging and biomaterials.

1.2 The objectives of this research

1. To prepare NRBC reinforced composite films via the latex solution process.
2. To improve the composite structural stability by the acid modification.
3. To investigate the characteristics of the films with the difference condition.

1.3 The scope of this research

1. The latex solution process as the method of NRBC blending was used in the preparation of NRBC composite films under conditions of no precipitate of BC fibers from the NR solution.

2. Effects of BC fiber contents that are 20, 50, and 80 wt.% in NRBC composites on the properties of films were studied.

3. Effects of the lactic acid modification on the properties of the composite films were studied.

4. The NR, BC, NRBC, and ANRBC composite films were characterized by;

- a. Scanning electron microscopy (SEM)
- b. Fourier transform infrared (FTIR) spectroscopy
- c. Particle size analysis with dynamic light scattering (DLS)
- d. The transparency and opacity testing
- e. The dynamic advancing and receding water contact angle analysis
- f. X-ray diffraction (XRD) analysis.
- g. Thermogravimetric analysis (TGA)
- h. Differential scanning calorimetry (DSC)
- i. Dynamical mechanical thermal analysis (DMTA)
- j. Tensile property testing
- k. The solvent uptake study

l. The water vapor transmission rate (WVTR)

m. Biodegradation in soil

n. Anti-microbial ability



CHAPTER II

BACKGROUND AND LITERATURE REVIEW

2.1 Natural rubber

Most of the NR is derived from the rubber tree *Hevea Brazilliensis* which originates from the Amazon River in South America. NRL is a white colloidal suspension which usually contain 30 wt.% of rubber particles. In addition, there are other components that shown in Table 2.1. The rubber particles are encompassed by molecule of protein and are effectively negatively charged. When opened to air, latex coagulation occurs while bacteria and enzymes rapidly decompose proteins, since crosslinking within the rubber particles leads to degradation of the rubber chains. The latex is then processed until centrifuged latex rubber concentration was increased to 60% as high concentrated rubber latex. Normally, the latex added with ammonia as preservation of their physical properties.

Table 2.1 Components of fresh NRL

Components	Concentration (wt.%)
Dry rubber contents	20-45
Protein constituents	1.5
Resin constituents	2.0
Carbohydrate constituents	1.0
Inorganic substances	0.5
Water	50-75

The NR polymer is nearly 100% cis-1,4-polyisoprene which molecular weight ranging from 200,000 to 500,000 daltons. Due to chemical structure of NR is non-polar molecule, so the solubility in non-polar solvent such as benzene and hexane is high whereas natural rubber less solute in high polar solvent.

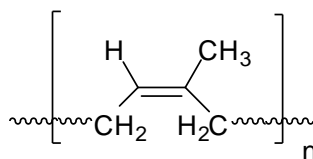


Figure 2.1 Chemical structure of cis-1,4-polyisoprene

In general, molecular structure of NR is arranged to be amorphous but it differs in aspect when the temperature decrease. The crystallization can occur at low temperature. A degree of flexibility was enhanced with the increase of temperature. Strain-induced crystallization is a result of significantly improved mechanical properties including tensile strength, tear resistance, and abrasion resistance. Another high elasticity is a highlight of NR properties that is the product quality requirements such as tires, gloves, food wrap, as well as plastic bags or flexible packaging. The elastic properties occur from their ability to stretch the chains apart, but when the tension is released the chains snap back to the original position. NR vulcanized by thermal energy, sulfur, or peroxide can prevent it from perishing. Moreover, vulcanized NR is also high resistance and elasticity due to vulcanizing system creates a cross-linking pattern. The development of vulcanized rubber for automobile tires greatly aided this industry.

2.2 Bacterial cellulose

BC is a product from primary metabolism processes of microbes such as Zoogloea, Sarcina, Salmonella, Rhizobium, Escherichia, Agrobacterium, Pseudomonas, Aerobacter, Achromobacter, Azotobacter, Alcaligenes, and Acetobacter. Usually, Acetobacter xylinum species were studied and used BC-producing. It was found to be superior to numerous accounts as compared with the plant one and is an obligate aerobic bacterium usually found in vinegar, alcoholic beverages, fruits, and vegetables. Acetobacter xylinum is a simple Gram-negative, rod shaped, and strictly aerobic bacterium, which has an ability to synthesize a large quantity of high-quality cellulose organized as twisting ribbons of microfibrillar bundles. Morphologically, the reproducible pellicle is obtained by controlling parameters of bacterial growth, for instance, the composition of the culture media, pH, temperature, and oxygen tension.

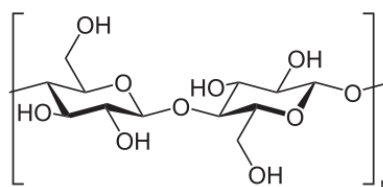


Figure 2.2 Chemical structure of BC

BC is polysaccharides with the formula $(C_6H_{10}O_5)_n$ which is a basic structural material of most plant substances, a molecule consisting of a long chain and glycosidic linkage. Therefore, it displays unique properties including high mechanical strength, high water absorption capacity, high crystallinity, and an ultra-fine and highly pure fibre network structure.

As a result of cellulose is biomaterials obtained from nature and renewable, it as additive substance, filler, or reinforcing reagent was always added to mix with plastics for cost reduction or increasing production. Moreover, the pretreatment like the removing of hemicellulose, pectin, and lignin was not necessary on mixing process, BC has attracted much attention in recent years because it has short time of synthesis and is not the cause of environment pollution.

2.3 Lactic acid

Lactic acid (2-hydroxypropanoic acid) is the simplest 2-hydroxycarboxylic acid (or a hydroxy acid) with a chiral carbon atom and exists in two enantiomeric forms including S-lactic acid and L-lactic acid.

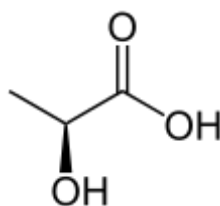


Figure 2.3 Chemical structure of lactic acid

The lactic acid molecule has a hydroxyl and an acid functional group, which may result of intermolecular and intra molecular esterification reactions. The first step is the formation of a linear dimer. This condensation reaction can proceed to higher oligomers and is promoted by removal of water. Also a cyclic dimer, lactide, is formed

in small amounts. Lactide can be formed by intra molecular esterification of lactoyl lactic acid or by breakdown of higher oligomers. Due to these reactions, a solution of lactic acid at equilibrium consists of monomeric lactic acid, dimeric lactic acid or lactoyl lactic acid, higher oligomers of lactic acid, and lactide. The ratios between all substances depend on the amount of water present; for example, a 90.1% lactic acid solution contains about 59.3% of monomeric lactic acid and 27.3% of lactoyl lactic acid and higher oligomers [28].

2.4 Polymer reinforcement

The reinforcement of polymer is the process of the property development which was used to improve the material performance. An initiation factor of reinforcement process is a reinforcing reagent. In the past, nanoscopic additives such as carbon black and silica nanoparticle were major reagents for polymer reinforcement. There are a several researches or study that the main aims are development of material performance via reinforcement process. The researches of natural rubber reinforcement were collected below Table 2.2 and 2.3.

2.4.1 Composite preparation

In general, there are two major method of composite material preparation including melt blending and solvent blending (solution blending). Melt blending is most environmental-friendly method for dispersion of fillers in the polymer matrix due to it is the absence of inorganic solvents and can be performed using scalable melt extrusion. These functions make this method is the leading process among other production processes and provide practical, cost-effective, and very gainful solutions of polymer composites industry. However, melt blending is particularly difficult for the extremely low bulk density because of the materials feeding into melt extruders is more difficult. Moreover, there are the limitations of a destruction of polymers because the high processing temperature melts polymer molecules into viscous liquid, generating rheological shear stress. In case of solvent blending, this method is probably the simplest method for introducing alternative properties or functions of the core

material due to it involves mixing of two parts in the solution. Colloids where one part is non-soluble such as carbon nanotubes and silica particles have been suspended in solution. Three solution blending behaviors are commonly occurred, first one is the materials for mixing are soluble in a common solvent, second one is that there is no common solvent to dissolve both materials and the third one is only material is insoluble as mentioned earlier. Given the performance of blending, combinations of the three actions may be used together in fiber spinning. Despite the ease of using blending to introduce a separate property to the material, a major limitation is the potential leaching of the added material since there is no chemical bonding between the base and added material. However, if the material lost is very slow or insignificant, the benefit of this method may outweigh this weakness [<http://electrospintech.com/>].

Kim et al., (2011) studied on the subject of the effects of polyethylene functionalization and blending methods on graphene-polyethylene nanocomposite properties. They reported solvent blending yielded better dispersion than melt blending. Moreover, modulus increased more for solvent mixed blends than when they were melt blended [29].

Ismail et al., (2013) studied the properties of halloysite nanotubes (HNTs)-filled NR prepared using different mixing methods. There are two methods including the melt mixing which was carried out by using a two roll mill model and the solution mixing that the mechanical stirrer was required to assist swollen process of NR in toluene. They found the solution mixing method caused longer in both properties and higher than mechanical mixing nanocomposites. Tensile strength and modulus of solution mixing nanocomposites was higher but lower than mechanical mixing nanocomposites at any HNTs loading. Inclusion of HNTs caused a reduction in swelling percentage, fatigue life but increased the thermal stability of both nanocomposites. Swelling percentage of solution mixing nanocomposites showed lower values than mechanical mixing nanocomposites at any HNTs loading. However, fatigue life and degradation temperature nanocomposites prepared by solution mixing were higher than mechanical mixing method [30].

2.4.2 Development of blending process

Immiscible behaviors of a blending compound such as the filler flocculation, aggregation, and coagulation are the limitations of composite preparation. There are several researches which were studied about the improvement of blending method to reduce these problems.

Watcharakul et al., (2011) studied on the object of NR reinforcement with silica nanoparticles. The study have three main methods to prepare silica nanocomposites including NR reinforcement with commercial silica, NR reinforcement with in situ silica which was synthesized via the sol-gel reaction of tetraethoxysilane (TEOS) and methyl methacrylate (MMA) grafted NR blended with in situ silica. They reported the comparisons of reinforcing efficiency of each method. The performance of in situ silica is higher than commercial silica due to in situ silica particles are smaller than commercial silica particles. A good dispersion is ability of small particles. NR grafting with MMA reduces the immiscible behaviors of blending and enhance the compatibility of NR and silica particles [7].

Soheilmoghaddama et al., (2013) studied on the object of epoxide NR (ENR) blending with regenerated cellulose. Regenerated cellulose (RC)/ENR blend films were prepared by coagulating with water. The result showed the existence of hydrogen bonds between hydroxyl groups of RC with ENR thereby suggesting interfacial interaction between RC and ENR. The crystallinity of the composites quite decreased with the increase in ENR composition. The thermal stability of RC greatly improved upon blending with ENR. The elongation at break of the blends was found to be more than pure RC while Young's modulus reduced with ENR content. The cellulose was toughened by the addition of ENR [31].

Trovatti et al., (2013) studied on the object of the preparation of NR reinforcement with nanocomposites including BC and BC coated with polystyrene (BCPS). The study was considered under the influences of four condition systems; NRBC nanocomposites, NRBCPS nanocomposites, vulcanized-NRBC (VNRBC) nanocomposites, and vulcanized-NRBCPS (VNRBCPS) nanocomposites. The use of both

BC and BCPS nanofibers as reinforcing reagent resulted in substantial improvements in the mechanical properties of NR and VNR matrices. In case of NRBCPS and VNRBCPS systems, the polymerization of styrene took place at the surface of BC nanofibers that is a cause of increment of compatibility between NR and BC. Vulcanization modifies chemical structure such as OH groups of cellulose exerted an important role with respect to the interaction among fibers, formation of intra- and intermolecular hydrogen bonds, and continuous structure inside the matrix .The highest of performance is VNRBCPS system [21].



Table 2.2 The researches of natural rubber reinforcement via melt blending

Reinforcing reagents	Procedure	Optimal loading contents	Properties improvement	Applications	Reference
Carbon nanotubes (CNT)-coated short jute fiber (JFs)	<ol style="list-style-type: none"> NR was cross-linked with ZnO and steric acid in two-roll mixing mill. The JF-CNT was added in the elastomer mixture followed by adding the accelerator and the sulphur. 	20 Phr	<ul style="list-style-type: none"> Mechanical and dynamic mechanical properties Lightweight materials 	<ul style="list-style-type: none"> Lightweight elastomer product 	[32]
Nanoclay	<ol style="list-style-type: none"> NR-SBR type rubber was mixed with curatives, carbon black, stabilizer, and process acids in a two roll mixer at 145°C. The mixture was mixed with nanoclay at 100-110 °C. 	2 wt.%	<ul style="list-style-type: none"> Modulus Hardness Thermal mass decomposition 	<ul style="list-style-type: none"> Automotive tyre Tyre based product 	[13]

Table 2.3 The researches of natural rubber reinforcement via melt blending (Continue)

Reinforcing reagents	Procedure	Optimal loading contents	Properties improvement	Applications	Reference
Oil palm ash	<ol style="list-style-type: none"> Mixing of NR and oil palm ash were don using two roll mill. Moulded sheets were conditioned in desiccators. 	-	<ul style="list-style-type: none"> Dynamic mechanical properties Mechanical properties 	<ul style="list-style-type: none"> Automotive tyre Tyre based product 	[4]
Corn flour particles	<ol style="list-style-type: none"> The dried NR blends with modified corn flour at 80 °C, and mixed at 60 rpm for 20 min. The mixture was then cooled to 80 °C, followed by the addition of sulfur and accelerator, and mixed for 3 min. 	20 wt.%	<ul style="list-style-type: none"> Tensile properties Level of oxidation 	<ul style="list-style-type: none"> Renewable rubber materials 	[33]

Table 2.4 The researches of natural rubber reinforcement via solution blending

Reinforcing reagents	Procedure	Optimal loading contents	Properties of composites	Applications	Reference
Exfoliated grapheme oxide (GO)	<ol style="list-style-type: none"> 1. NRL were added GO at ambient temperature. 2. The solution is then left to dry at ambient temperature. 	0.75 wt. %	<ul style="list-style-type: none"> • Stiffness • Strength • Modulus • Thermal stability 	<ul style="list-style-type: none"> • Lightweight elastomer product • Automotive tyre • Tyre based product 	[29]
Organically modified montmorillonite (OMMT)	<ol style="list-style-type: none"> 1. OMMT was swelled in water under stirring to obtain a suspension. 2. NRL was added to the suspension, followed by ultrasonication. 3. The NR/OMMT emulsion was removed by freezing. 4. Composites were dried in the oven. 	5 wt. %	<ul style="list-style-type: none"> • Tensile strength • Crystallization 	<ul style="list-style-type: none"> • Pneumatic tires • Rubber bearings 	[34]

Table 2.5 The researches of natural rubber reinforcement via solution blending (Continue)

Reinforcing reagents	Procedure	Optimal loading contents	Properties of composites	Applications	Reference
Banana fibers	<ol style="list-style-type: none"> 1. NRL was prevulcanized 2. The solution was added with banana fiber 3. Mixing is in the ball milling process 4. The suspension poured in glass plates and dried in the oven. 	4.5-5.9 wt. %	<ul style="list-style-type: none"> • Membrane transport • Rheological properties • Thermal degradation 	<ul style="list-style-type: none"> • Barrier membrane 	[35]
Clay	<ol style="list-style-type: none"> 1. Clay was added progressively to the latex while stirring. 2. Water was removed at 60 °C under reduced pressure. 3. Dried in an oven under air at 60 °C (at least 48 h). 	-	<ul style="list-style-type: none"> • Mechanical properties • Structural properties 	<ul style="list-style-type: none"> • Automotive tyre • Tyre based product 	[36]

2.5 Cross-linked NR

NR and some other polymers can be cross-linked. A chemical reaction takes place that connects the chains to each other permanently. This makes the whole structure more rigid and less elastic. It also makes the polymer a lot stronger and harder. Vulcanized rubber is cross-linked using sulfur, results from the introduction of short chains of sulfur atoms that link the polymer chains in NR. As the number of cross-links increases, the polymer becomes more rigid. The decision to classify a polymer as branched or cross-linked is based on the extent to which the side-chains on the polymer backbone link adjacent polymer chains. The easiest way to distinguish between these categories is to study the effect of various solvents on the polymer. Branched polymers are often soluble in one or more solvents because it is able to separate the polymer chains. Cross-linked polymers are insoluble in all solvents because the polymer chains are tied together by strong covalent bonds. Linear and branched polymers form a class of materials known as thermoplastics. These materials flow when heated and can be molded into a variety of shapes which they retain when they cool. Heavy cross-linking produces materials known as thermoset plastics. Once the cross-links form, these polymers take on a shape that cannot be changed without destroying the plastic [<http://www.rsc.org/>].

Georjon et al., (1996) studied on the object of the effects of crosslink density on mechanical properties of high glass transition temperature (T_g) polycyanurate networks. Networks with a variable extent of reaction were studied; the variation of the cyanate conversion (0.8 to 1) corresponds to a variation of T_g (150–290°C) and crosslink density. The deformations and the fracture toughness were studied at ambient temperature and related to the network structural parameters. They reported the decrease of the Young's modulus with an increase in conversion that is a result of two facts. First, the cohesive energy density was lower in the more cross-linked networks. And second, the T_g were higher in the network of high crosslink density [37].

Visakha et al., (2012) studied the effects of cross-linked NR nanocomposites reinforced with cellulose whiskers isolated from bamboo waste on mechanical and

thermal properties. The reinforcing reagents were prepared by cellulose nanowhiskers (CNWs) that were extracted from bamboo pulp residue of newspaper production. The coagulated NRL containing bamboo CNWs was compounded with solid NR and vulcanizing agents using a two-roll mill. Curing was carried out at 150°C for 9 min. The addition of CNWs had an advantageous impact on the tensile strength, elastic modulus, storage modulus, tan delta peak position and thermal stability of the cross-linked NR. Theoretical modeling of the mechanical properties showed a lower performance than predicated and therefore further process optimization and/or compatibilization are required to reach the maximum potential of these nanocomposites. The higher strength and the modulus of the matrix materials in the current are due to the crosslinking of NR as well as the processing method used. Despite the moderate increase in tensile strength and modulus, the behavior of the curve is not changed by the addition of CNWs indicating that the effect due to crosslinking of NR predominates over the reinforcing effect of CNWs [38].

Chen et al., (2014) studied on the object of preparation of a bio-based material, dynamically vulcanized polylactide (PLA)/natural rubber (NR) blend in which the cross-linked NR phase owned a continuous network-like dispersion. In this study, by using a crosslinking reagent, dicumylperoxide (DCP), and a dynamic vulcanizing technique, a greatly toughened bio-based PLA/NR blend material was prepared by melt blending in a system at 150°C and at a rotor speed of 60 rpm. The dynamic vulcanization refers to a process of selectively vulcanizing rubber phase during melt blending with a thermoplastic polymer, leading to a two-phase material in which the cross-linked rubber phase is usually in particulate forms dispersed in the plastic matrix. In summary, they reported a super toughened PLA/NR blends prepared via a dynamic vulcanizing technique, in which the cross-linked NR phase owned a continuous network-like dispersion. PLA grafting onto NR during melt-blending results in a significantly improved interfacial compatibilization as a result of their high performance. The dynamic vulcanization of PLA/NR blend materials show promise for development in various functional applications [39].

CHAPTER III

EXPERIMENTAL

3.1 Materials

NRL 60 DRC were purchased from the Rubber Research Institute of Thailand. BC (98-99% water content in wet weight) was kindly provided by Pramote Thamarat (Institute of Research and Development of Food Product, Kasetsart University). All other chemical reagents were purchased from Sigma-Aldrich.

3.2 Bacterial cellulose preparation

The small cubes of BC hydrogel (size 1 cm × 1 cm × 1 cm) were purified by washing with deionized (DI) water, then were soaked with 1 wt.% NaOH for 48 hours to remove bacterial cells, and were rinsed with DI water until the pH was 7.0. To prepare BC slurry, BC was thoroughly crushed and homogenized by using a blender at room temperature.

3.3 Preparation of NRBC composites

BC slurry, cell removed, was added into NRL and the mixture was mechanically stirred for 5 minutes at room temperature. The mixtures were prepared with the compositions of BC/NR at 20/80 (NRBC20), 50/50 (NRBC50), and 80/20 (NRBC80). NRBC composite films were prepared by pouring BC/NR mixtures into a tray or plastic culture dish and then aging at room temperature for 3 hours. Finally, these films were dried in an air convection oven at 50°C over 2 days.

3.4 Modification of NRBC composites films via crosslinking process with organic acid

NRBC dried films were immersed in 0.25 M lactic acid for over 2 hours at ambient temperature. Then modified films were dried in an air convection oven at 50°C over 24 hours.

3.5 Characterization of the BC slurry

3.5.1 SEM

Scanning electron microscopy (SEM) micrographs were taken with a scanning electron microscope (model JSM-5410LV, JOEL, Tokyo, Japan). BC slurry was dried and then the dried samples were sputtered with nearly 200 Å of gold in a Balzers-SCD 040 sputter coater (Liechtenstein). The images were immediately viewed at a magnification of 20,000X and an accelerating voltage of 1.00 kV.

3.5.2 Particle size analysis with DLS

Particle size analysis of blended BC particles in DI water were performed using DLS on a Malvern Zetasizer Nano-ZS Version 7.04 (Malvern Instruments, Malvern, UK). Particle size and size distribution (PDI) were measured at 25°C.

3.6 Characterization of the NR, BC, NRBC and ANRBC films

3.6.1 SEM

SEM micrographs were taken with a scanning electron microscope (model JSM-5410LV, JOEL, Tokyo, Japan). The NRBC film was frozen in liquid nitrogen, immediately snapped, and then vacuum-dried. The free surfaces were sputtered with gold and photo-graphed. SEM was obtained at 15 kV.

3.6.2 FTIR spectroscopy

FTIR spectra of the films were measured at wave numbers ranging from 4000 cm^{-1} to 400 cm^{-1} at a resolution of 4 cm^{-1} with a Nicolet (US) SX-170 FTIR spectrometer.

3.6.3 The transparency and opacity testing

The opacity of the typical NR, BC and NRBC composite films were measured by using the UV-Vis Spectrophotometer (UV-2450, Shimadzu, Japan). Light transmission barrier properties were determined by measuring their light absorption at 600 nm (A_{600}). The degrees of opacity were the average values determined from 3 samples. The opacity were calculated as follows: [40, 41]

$$Opacity = \frac{A_{600}}{Thickness(mm)}$$

3.6.4 The dynamic advancing and receding water contact angle analysis

The dynamic advancing and receding water contact angle under air at room temperature were measured by using a contact angle goniometer (Ramé-hart. Instrument Co., USA, model 100-00), equipped with a Gilmont syringe and 24-gauge flat-tipped needle.

3.6.5 XRD analysis

The definitive structural information, crystallinity, interatomic distances and bond angles were characterized by X-ray diffraction analysis. XRD patterns of the materials were determined with a diffractometer (Bruker AXS Model D8 Discover). The operation conditions were as follows: power 40 kV and 30 mA. X-ray diffraction measurements were performed in the 2θ range of 5–40 using Cu K α radiation. The percentage of crystallinity were obtained from the X-ray empirical method proposed by Segal et al [42].

3.6.6 TGA

TGA was performed on a TGA Q50 V6.7 Build 203. Universal V4.5A TA Instruments, equipped with a platinum cell. The scanning range was 30–600°C using a heating rate of 10°C min⁻¹. The temperature for different percentages of weight loss, temperature at maximum decomposition and residue level at 600°C of NRBC composite films were measured from the TGA curves.

3.6.7 DSC

Performance of NRBC composite films such as thermal phase change, T_g , crystalline melt temperature (T_m), and thermal Stability were measured by DSC. Sample about 3-5 mg was sealed in aluminum pan. Then sample was subjected to DSC measurement under nitrogen atmosphere. In addition evaluate the curing behavior, non-isothermal DSC analysis of samples was carried out using NETZSCH DSC 204 F1 Phoenix. The thermal scanning were heated up from -100 to 300°C and with a heating rate of 10 °C/min.

3.6.8 DMTA

DMTA of the composite films were carried out using a NETZSCHDMA 242 equipment working under nitrogen atmosphere in the tension mode. The measurements were performed at a constant frequency of 1 Hz, amplitude of 30.00 μm , in the temperature range from -100 to 100°C and a heating rate of 5 K min^{-1} .

3.6.9 Tensile property testing

For tensile property testing, NRBC films were cut into strip-shaped specimens 1 cm wide and 10 cm long. The maximum tensile strength and break strain of NRBC composite films were determined with a Lloyd 2000R (Southampton, UK) universal testing machine. The test conditions followed ASTM D882. The tensile strength and break strain were the average values determined from 5 specimens.

3.6.10 The solvent uptake study

For solvent uptake, NRBC and ANRBC composites were determined at room temperature according to ASTM D471. Each test specimens were in the form of 2 x 2 cm^2 . The weight of each samples were measured before immersed into toluene and water for 1, 2, 3, and 4 weeks. The degree of swelling was calculated as;

$$\text{Degree of swelling (\%)} = \frac{W_w - W_d}{W_d} \times 100$$

where W_w and W_d denoted the weight of wet and dry membrane, respectively.

3.6.11. WVTR

WVTR of the NRBC and ANRBC dry films were determined with a water vapor permeation tester; Labthink Model W3/031. The test conditions followed ASTM E 96-00 Water vapor transmission of Material. WVTR testing was analyzed under 38°C and 90% relative humidity. The principle of this measurement was similar to that of conventional method that one side of the film was exposed to water vapor. As water solubilized into the film and permeated through the sample material and nitrogen gas swept and transported the transmitted water vapor molecules to a calibrated infrared sensor on the other side. Thereafter, a transmission rate was determined.

3.6.12 Biodegradation in soil

Biodegradation of NRBC and ANRBC composites in soil was carried for 6 months. Each test specimens were in the form of 5 x 5 cm² and buried in the pots of the soil to a depth of 10 cm under uncontrolled composting conditions. Temperature and humidity change as the weather during the day. The samples were weighed after 1, 3, and 6 months. For calculation of weight loss, the samples were carefully taken out, washed with distilled water, and dried at 50 °C for 24 h and then weighed. The specific biodegradation rates based on the mass loss of films were calculated according to below formula;

$$\text{Biodegradation (\%)} = \frac{W_1 - W_2}{W_1} \times 100$$

where W_1 is the initial dry weight of the samples (g) while W_2 is the dry residual weight of the samples after biodegradation in soil.

3.6.13 Anti-microbial ability

For anti-microbial ability, Escherichia coli (E. coli) and Staphylococcus aureus (S. aureus) were used for the antibacterial tests of the NRBC and ANRBC films. Each microbe was suspended in broth at the standardized concentration of 10⁸ cells/mL prior to spreading 1 mL broth onto the agar plate. Subsequently, the film samples were cut into 1 cm circular discs. These films were gently placed onto the colonized

agar plate. NR film was used as a negative control. These plate were incubated at 37°C for 24 h. The clear zone was determined.



CHAPTER IV

RESULTS AND DISCUSSION

4.1 Characterization of the BC slurry

4.1.1 Scanning electron microscopy (SEM)

Cubic pieces of BC (1cm x 1cm x 1cm) were thoroughly crushed and homogenized by a blender as the biodegradable filler materials for the reinforced NR composite preparation. The freeze-dried BC slurry were characterized by SEM as shown in Fig.4.1, a rod-shaped fibril of BC was in form of small sheet composed of nanofiber networks, in which the diameters of the fibers were around 3-8 nm [43-45]. According to the SEM image of BC sample, it shown the oriented discontinuous fibers.

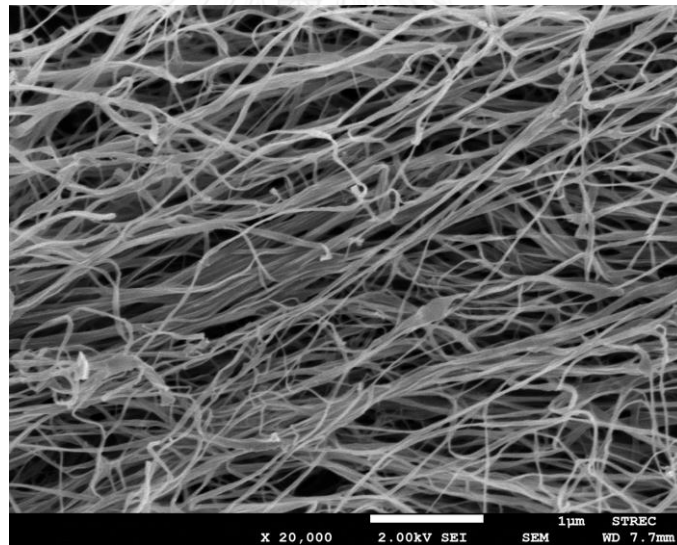


Figure 4.1 SEM image of BC in the slurry

4.1.2 Particle size analysis with dynamic light scattering (DLS)

Particle size distribution of BC fiber analyzed by Zetasizer Instruments is shown in Fig.4.2. The particle size distribution measured by number distribution, showed an average size of 1.249 μm with a polydispersity index (PDI) of 0.910. Comparing with the fiber size in the SEM images, the length of the particles is usually larger than their

exact diameter due to the presence of stabilizing molecules on the surface of the particle [46].

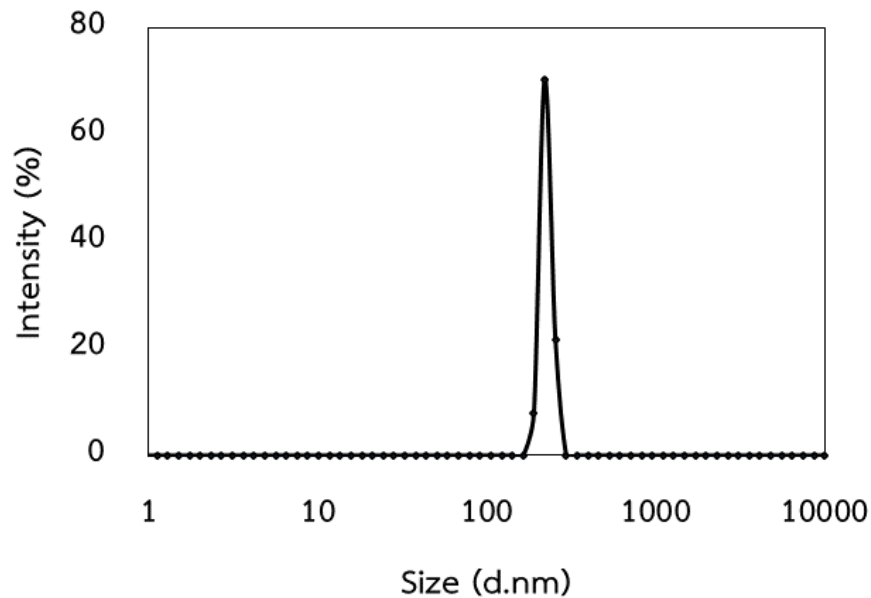


Figure 4.2 Particle size distribution of BC fiber

4.2 Characterization of the NR, BC, NRBC and ANRBC films

4.2.1 Scanning electron microscopy (SEM)

The outer surface and cross-section morphologies of NR (Fig. 4.3A and 4.3C) and BC (Fig. 4.3B and 4.3D) was employed to study by SEM. Both have a relatively smooth outer surface but the NR present the glossy and gritty films while dried BC is light-impervious films. In case of cross-section surface, smooth surface of NR which was broken in a liquid nitrogen freezing chamber have some fracture while the cross-section of BC presents a compact layered structure or laminated structure which occupies pore space between each fiber layers.

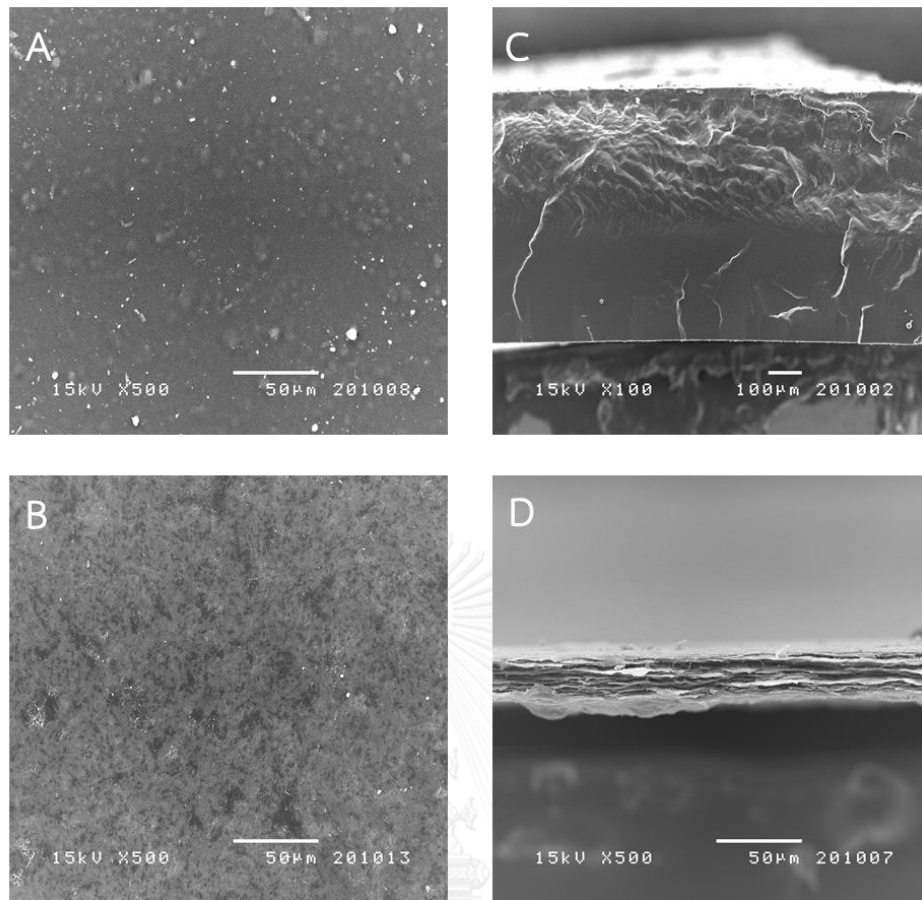


Figure 4. 3 On the left, SEM images of the films of NR (A) and BC (B); on the right, enlarged view of the cross section of NR (C) and BC (D)

Compatibility and the phase structure between BC fibers and NR in the composite matrix were studied by SEM of the cross-section morphologies of the composite films (Fig.4.4A-C): NRBC20 (Fig. 4.4A), NRBC50 (Fig. 4.4B) and NRBC80 (Fig. 4.4C). SEM images of the cross section of the NRBC composite films show the characteristics of two immiscible components with the well dispersion and well distribution of BC fibers in NR matrix without extensive agglomeration and the BC filler precipitation. The NRBC20 composite film has the smoothest surface when comparing with other NRBC composite films. The BC adding in NR matrix was suggested to arise the agglomeration of filler fibers due to the high polar interaction as well as the disorder of BC fibers that is the cause of the reduction of the compatibility and BC fiber dispersion. Moreover, total pore volume increases with the increasing of the BC laminated structure in the composite matrix. The layered structures were apparently

displayed in BC film and NRBC films of BC loading content at $\geq 50\%$. For ANRBC composite films (Fig.4.4D-F): ANRBC20 (Fig. 4.4D), ANRBC50 (Fig. 4.4E) and ANRBC80 (Fig. 4.4F), there are similar appearances with definite NRBC composite films. These indicate both of NR and BC were not dissolved in lactic acid as well as the composite structure were not destroyed or swollen after acid modification process.

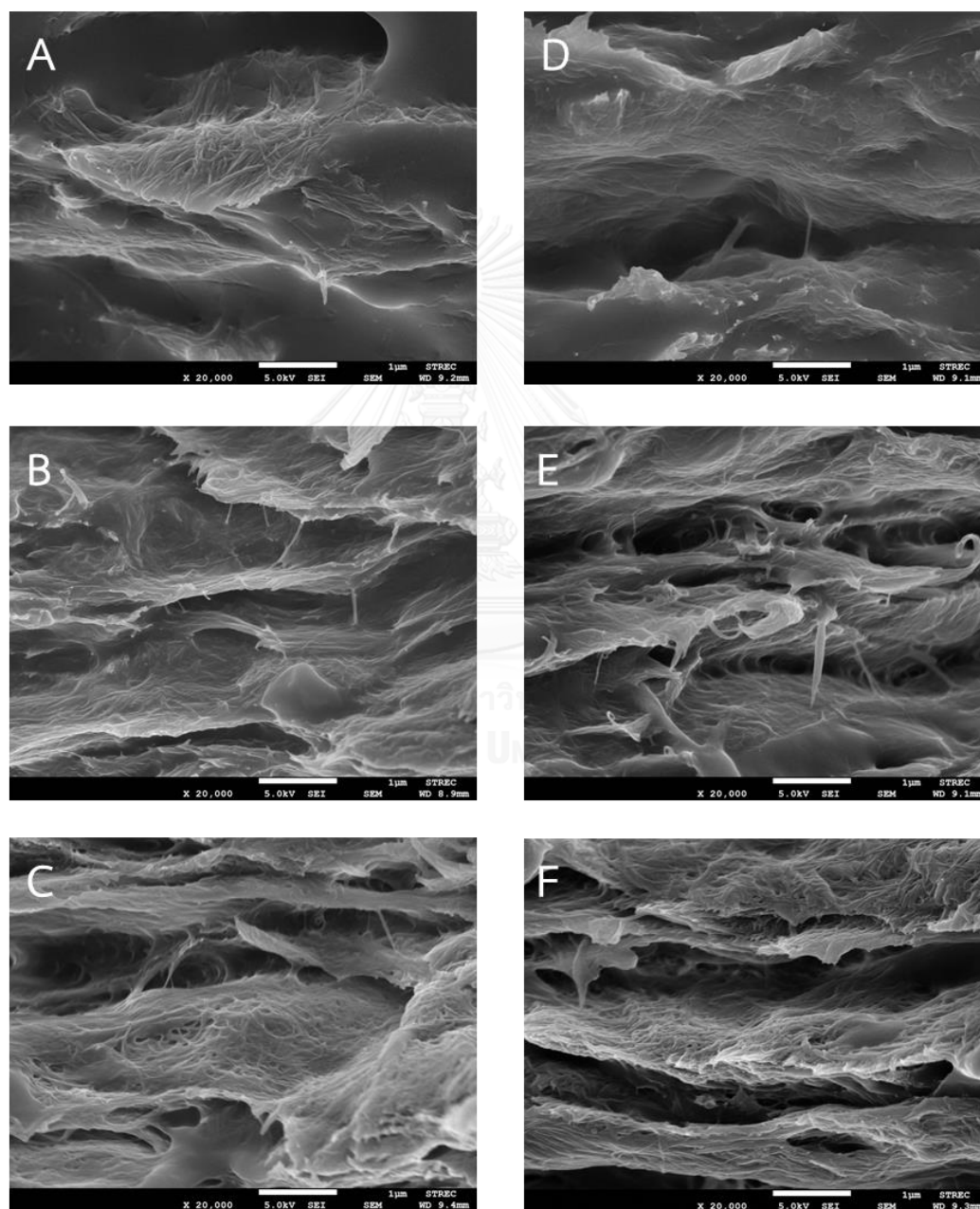


Figure 4.4 SEM images of the cross section of NRBC20(A), NRBC50(B), NRBC80(C), ANRBC20(D), ANRBC50(E), and ANRBC80(F)

4.2.2 Fourier transform infrared (FTIR) spectroscopy

Chemical interaction between NR and BC was determined by FTIR spectroscopy. According to the FTIR spectra (Fig.4.5), pure NR adsorbed at 2896 and 2925 cm^{-1} are assigned to asymmetric stretching vibration of methyl ($-\text{CH}_3$). In addition, it is appeared a peak of symmetric stretching vibration of methylene ($-\text{CH}_2$) at 2842 cm^{-1} . The C=C stretching is situated at 1652 cm^{-1} . In case of pure BC, there are a peak of O-H stretching of hydroxyl group at 3000-3600 cm^{-1} , symmetric stretching vibration of methylene ($-\text{CH}_2$) at 2866 cm^{-1} , C-O-C pyranose skeletal vibration at 1035 cm^{-1} as well as a peak of C-O symmetric stretching of primary alcohol at 996 cm^{-1} . Disappearance of some peaks in the spectra which were shown in FTIR spectra of raw plant cellulose because BC do not contain hemicellulose and lignin [47]. For the NRBC composites, their FTIR spectra show the consisting of pure NR and BC peaks which were including around 2896 cm^{-1} , 2925 cm^{-1} and 1652 cm^{-1} are assigned to $-\text{CH}_2$, $-\text{CH}_3$ and C=C stretching respectively. Moreover, there are a peak of O-H stretching at 3000-3600 cm^{-1} and a peak of C-O stretching at 996 cm^{-1} . For the effects of BC fiber content on the patterns of functional groups and chemical interaction between NR and BC in the NRBC composites, it was shown that the peak area of OH groups were enhanced with the increase of BC fiber content, whereas peak areas of methyl and methylene groups were decreased and the position of characteristic peaks of composites slightly shifted from peaks of pure NR and BC, which implied some interactions without chemical bonding between BC fibers and NR matrix. For the acid modification, ANRBC have the closely identical pattern, intensity and position of characteristic peaks of NRBC composites. These indicate the acid modification did not lead to form the strong chemical bonding, associated with the sharing or transfer of electrons between the participating atoms. However, it might be occur the NR-BC interaction such as hydrogen bond which the FTIR spectroscopy cannot detect.

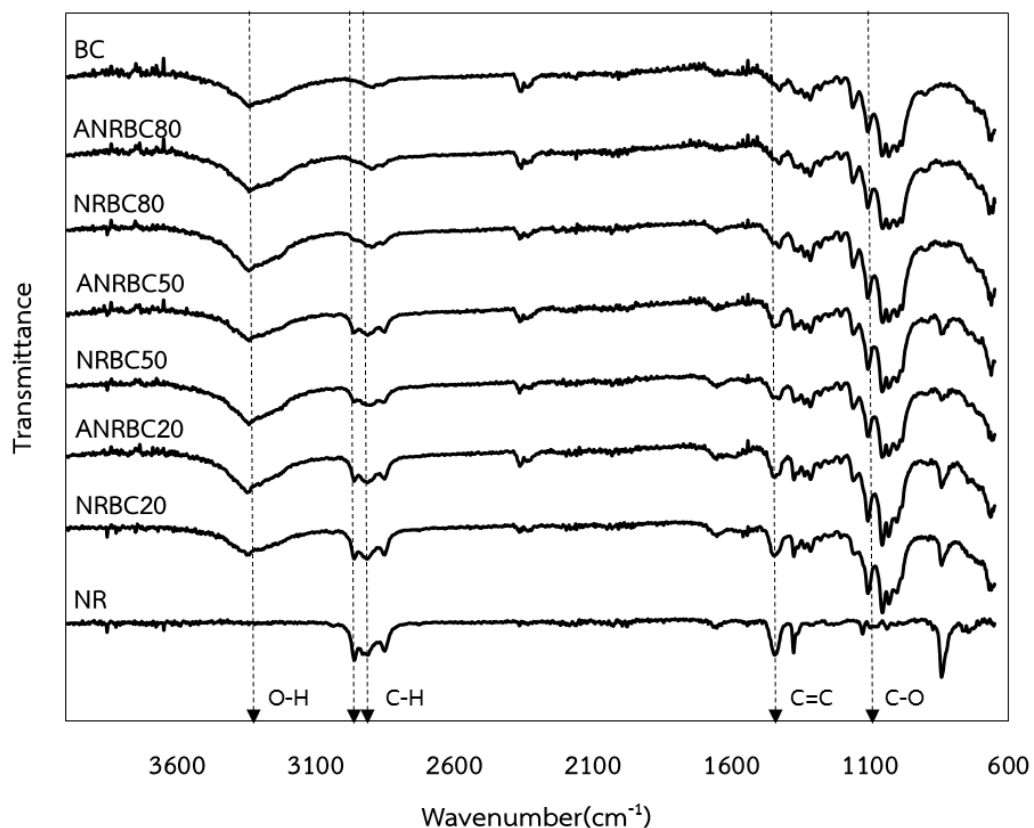


Figure 4.5 FTIR spectra of NR, BC, NRBC and ANRBC composites

4.2.3 The transparency and opacity testing

For packaging applications, the transparency and opacity of films are important factor as it affects the visibility of the packaged product to consumers [48]. For this study, the degree of opacity was only determined because the effects of the film thickness can be neglected for the opacity calculation. Opacity is a measure of the degree to which light is not allowed to pass through it that measured by the UV-Vis Spectrophotometer. According to Fig.4.6, the opacity of pure NR and BC were 1.31 and 33.10, respectively. For the NRBC composites, the degree of opacity of films increased proportionally to the increase of BC fiber content. This is because the incorporation of BC was in form of a network structure into the NR matrix as well as the distribution of BC fibers in NR. For ANRBC films, the density of NR and BC were less changed after acid modification when comparing with NRBC films. These also indicate NR and BC were

not dissolved in lactic acid as well as the composite structure were not destroyed in the acid modification process.

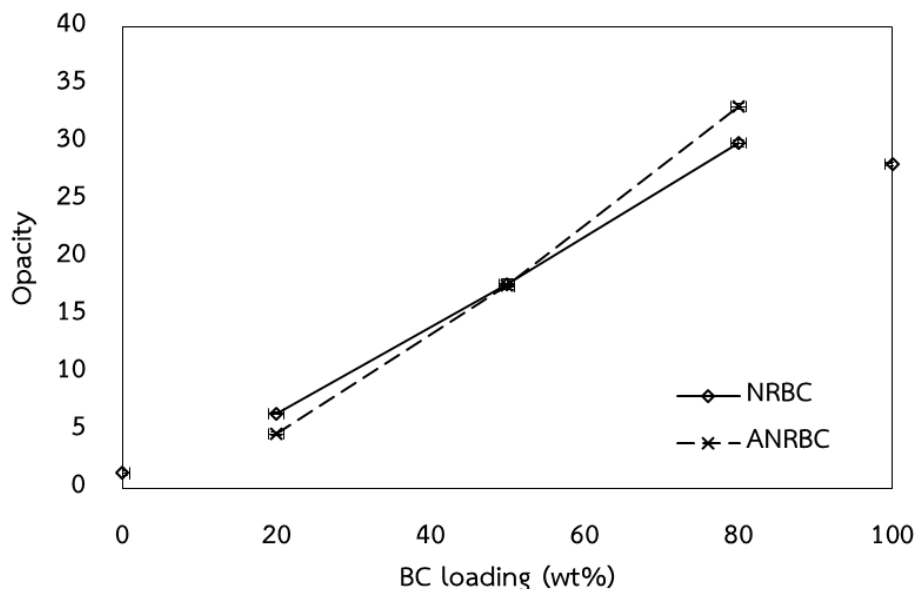


Figure 4.6 The opacity of NR, BC, NRBC, and ANRBC films

4.2.4 The dynamic advancing and receding water contact angle analysis

The material hydrophilicity was determined by measuring the water contact angle of the films. Generally, the materials which are rich in OH groups would present the high hydrophilic characteristics [49]. And BC is considered to be a hydrophilic substance. According to Fig.4.7, the water contact angle of BC was shown around 47.5 ± 2.8 while NR was around 116.2 ± 7.8 that indicates NR is a hydrophobic substance. For NRBC films, the dynamic water contact angle decreased with the increase of BC fiber contents due to the enhancing of OH groups on the surface of the composite films, resulting in higher hydrophilicity. In addition, the surface roughness as the surface morphology change might affect the value of contact angle. The water contact angle could be decreased with the increasing surface roughness as well as the total pore volume in the composites[50]. These are also in the plant cellulose behaviors that was reported in the previous study [51].

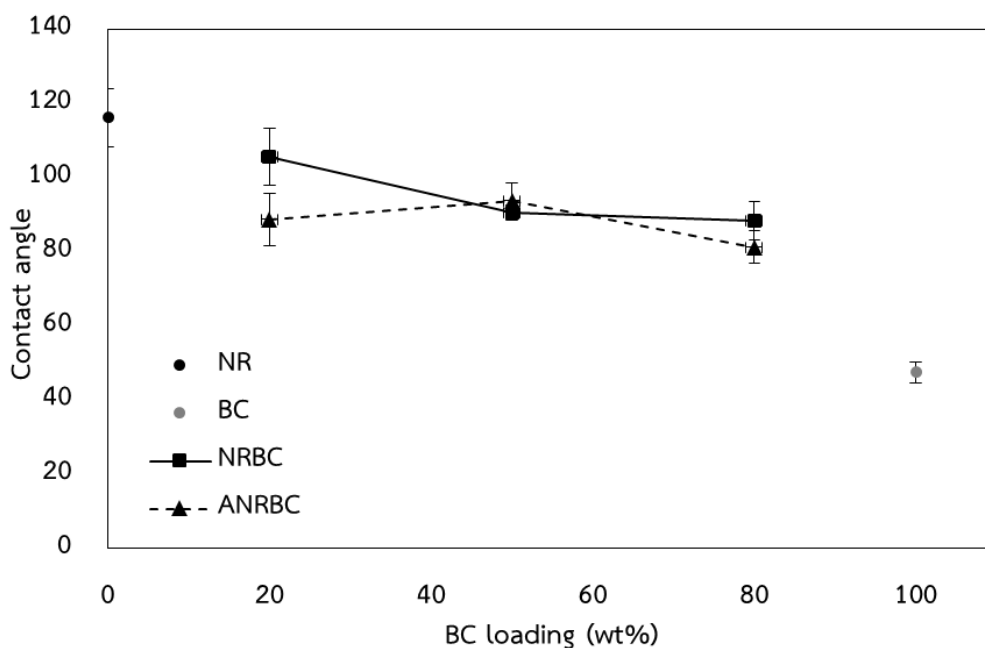


Figure 4.7 Dynamic water contact angle of NR, BC, NRBC and ANRBC composites

In part of acid modification, the water contact angle remains nearly constant, at 81-93°. Hence, the amount of OH groups on the surface of the ANRBC films was not changed with the acid modification even the hydrophilic polymer surface can thus be generated by acid treatment. OH group of cellulose structure can be translated to cellulose ester by the esterification reaction with carboxylic acid [52]. However, the esterification reaction was occurred under high temperature with the acceleration agent. For room temperature and without catalyst that accelerates a chemical reaction condition, OH groups on the chain of BC fibers could be able to form hydrogen bonds with lactic acid according to Fig.4.8. Therefore, the physicochemical characteristics of the acid modified surfaces, including surface compositions and polarity as well as the hydrophilicity, had the effects of hydrogen bond formation. The excess acid was cause of the tiny difference of polarity of each acid modified composite. However, there are some amounts of molecules of lactic acid which insert onto the composite surface when compared with the volume of NR and BC. The slightly variance of the hydrophilicity could be explained with the existence of carbonyl and carboxyl groups on the surface. The interaction between lactic acid and BC which occur via acid

modification might promote the inter-intra molecular interaction of OH groups on BC fibers.

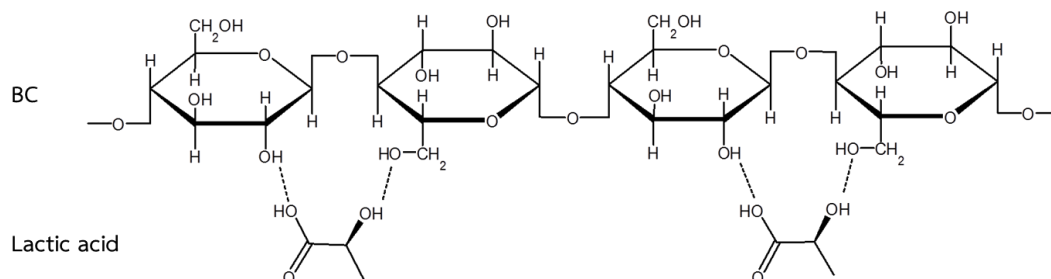


Figure 4.8 The interaction formation of the acid modification with lactic acid

4.2.5 X-ray diffraction (XRD) analysis

Generally, the material crystallinity was determined by XRD analysis. The XRD patterns of NR, BC, NRBC, and ANRBC composite films are shown in Fig.4.9 that shown the XRD pattern of BC demonstrated the peaks observed at 14.1°, 16.1° and 22.4°. These values supported the results in the previous study [53-55]. Comparing between pure BC fibers and the others, the degree of crystallinity of BC (58.18%) is higher than plant cellulose [56]. XRD patterns of amorphous polymer have a very distinct strong and broad shape like the peak of NR while the XRD patterns of composite films shown all of position are similar in appearance of BC pattern. The diffraction peaks of BC were relatively sharp and high density hence it is critical to maintain the highest crystal structure purity. The ordered crystalline arrangements in the cellulose appears due to the formation of inter-intra molecular hydrogen bonding by the OH groups. The hydrogen bonding restricts the free movement of the cellulosic chains and chains align close together in an orderly manner which tends to have the crystallinity. These are the cause that the NRBC composites shown the intense sharp peak when BC adding. Adversely, NR that was added into BC slurry under 20% BC loading for NRBC20 condition is the partial destruction of the original crystalline of BC fibers. This is the cause that NRBC20 shown the lowest degree of crystallinity with 17.91% when compared with others. Moreover, crystallinity dependent on the ability of the chains to form crystals and the mobility of the chains during the crystallization process [57]. In addition, the XRD patterns depend on the ordered crystalline arrangements.

According to XRD pattern, there are slightly difference between NRBC and ANRBC composites. This demonstrated that they have similar lattice structure, atom or molecule that has a three-dimensional ordered arrangement of basic units but it could be had the change in the large scale. Lactic acid cannot generate a new structure or destruct the original lattice structure under mild condition with the acid modification process. It is able to see that the degree of crystallinity of NRBC and acid ANRBC films was slightly different that were shown in Fig.4.10. This slightly difference was suggested by the amount variance of OH group that had the effect of hydrogen bond formation. For the composites with 80% BC loading, the degree of crystallinity was increased after acid modification. These results confirmed the presence of the hydrogen bond interaction between lactic acid and OH groups on the composite surface that there are large amount in NRBC80. This rearrangement of the hydrogen bond network within cellulose lead to the crystalline arrangements of the composite structure. Thus, ANRBC80 shown the highest crystallinity.

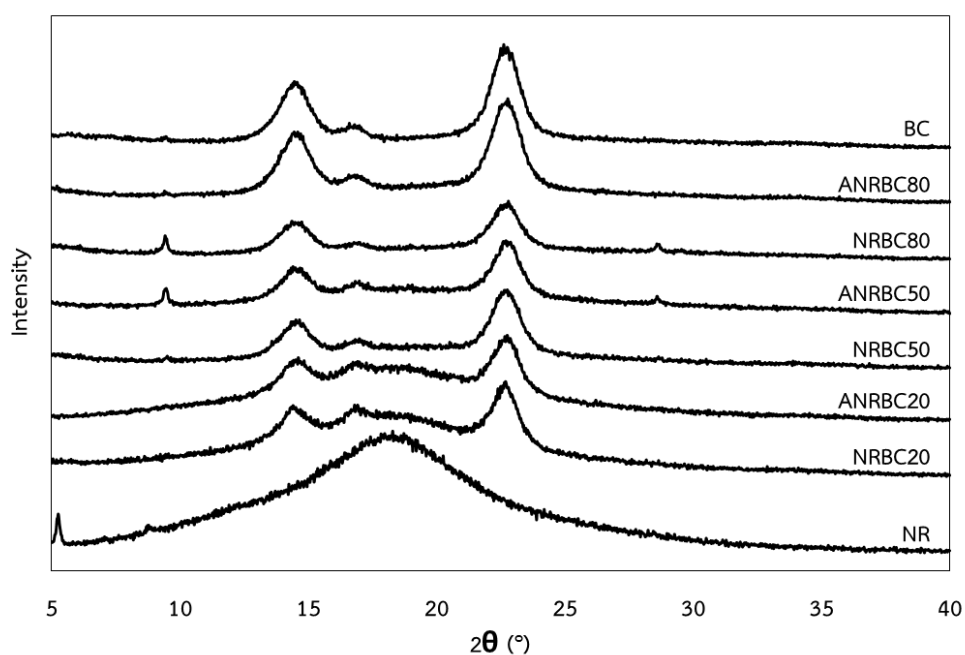


Figure 4.9 XRD patterns of NR, BC, NRBC and ANRBC composites

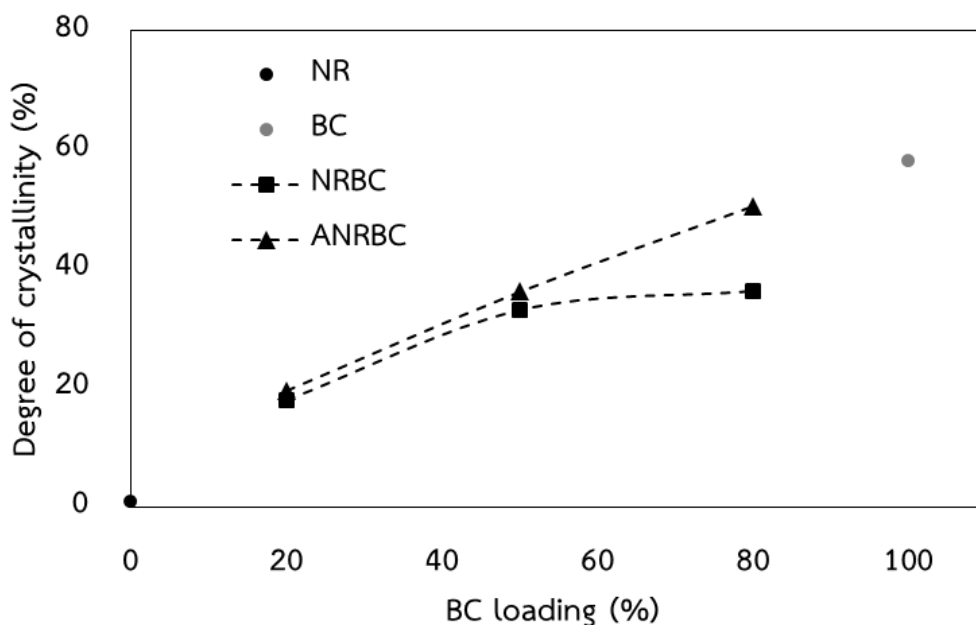


Figure 4.10 Degree of crystallinity of NR, BC, NRBC and ANRBC composites

4.2.6 Thermogravimetric analysis (TGA)

The thermal degradation of the NR, BC, NRBC, and ANRBC films have been investigated in terms of percentage weight loss with temperature. Degradation of polymers indications chain scission, cross-link formation, and cross-link breakage [35]. When the films were heated at low temperature, volatile components such as moisture or solvent would evaporate first. On heat adding, the polymer part would degrade and converse into gaseous products. Then the heating will remove all organic matter. And finally, there would be the residuals of inorganic fillers in the composites [38]. The TGA curves of BC, NR and NRBC, and ANRBC films are shown in Fig.4.11A. The peak at 59°C of BC was for the evaporation of water, which was account for 15% of the initial weight. The decomposition temperatures were 230 to 300°C and 230 to 490 °C for BC and NR films, respectively. For BC, this decomposition is the present of the breakdown of glycosidic linkages. In case of the composites, each films show peaks of the initial degradation after water evaporating like NR. For NRBC 20, the decomposition temperatures of polymers were observed to be enhanced as compared to pure NR and the other NRBC composites, which could indicate the better thermal stability at this composition as the results of NR-BC adhesion, NR-BC compatibility, composite

homogeneity and the small total void volume in the composite matrix. BC loading content at 20 wt.% were well dispersed and well distributed in the NR matrix that lead to the high heat resistance and thermal stability of the composites due to the reduction of the diffusion rates of volatiles out of the material [58, 59]. Further heating would remove all organic matters, giving the weight of residual char. The char yields of NR, NRBC 20 were lower as compared to NRBC50, NRBC80 and BC. When heated up to 580°C, the char yields of NR, NRBC20, NRBC50, NRBC80 and BC were 8.96%, 10.33%, 18.83%, 13.22%, and 18.86%, respectively. Similar TGA patterns of NR, cellulose and their composites were previously reported in the study of NR reinforced with nanocelluloses isolated from raw jute fibers by steam explosion process [35, 38]. In case of the acid modification, there less difference between NRBC and ANRBC patterns of TGA curves. These indicate the acid modification had slightly effect on the composite thermal stability because the lactic acid which were formed hydrogen bonding with OH groups on BC fibers suggested the promoting of OH inter and intra molecular structure of BC fibers in the composite matrix. This is the cause of the enhancing of structural stability of the composites. Thus, the thermal stability was improved after acid modification.

BC shown DTG pattern in Fig.4.11B like the plant celluloses that were previously reported [56, 60]. Meanwhile, the degradation of pure NR starts at about 220°C and was completed at 450°C that was also previously reported [61]. For NRBC and ANRBC composites, there are no separate degradation step that indicates that BC fibers have been completely mixed into the NR matrix. In addition, the acid modification can enhance the formation of inter and intra molecular hydrogen bonding of BC whisker in the NR matrix that lead to enhance the composite homogeneity. This were recognized with the sharp narrow peaks that confirmed the rearrangement of the hydrogen bond network within cellulose order crystalline arrangements of the composite structure.

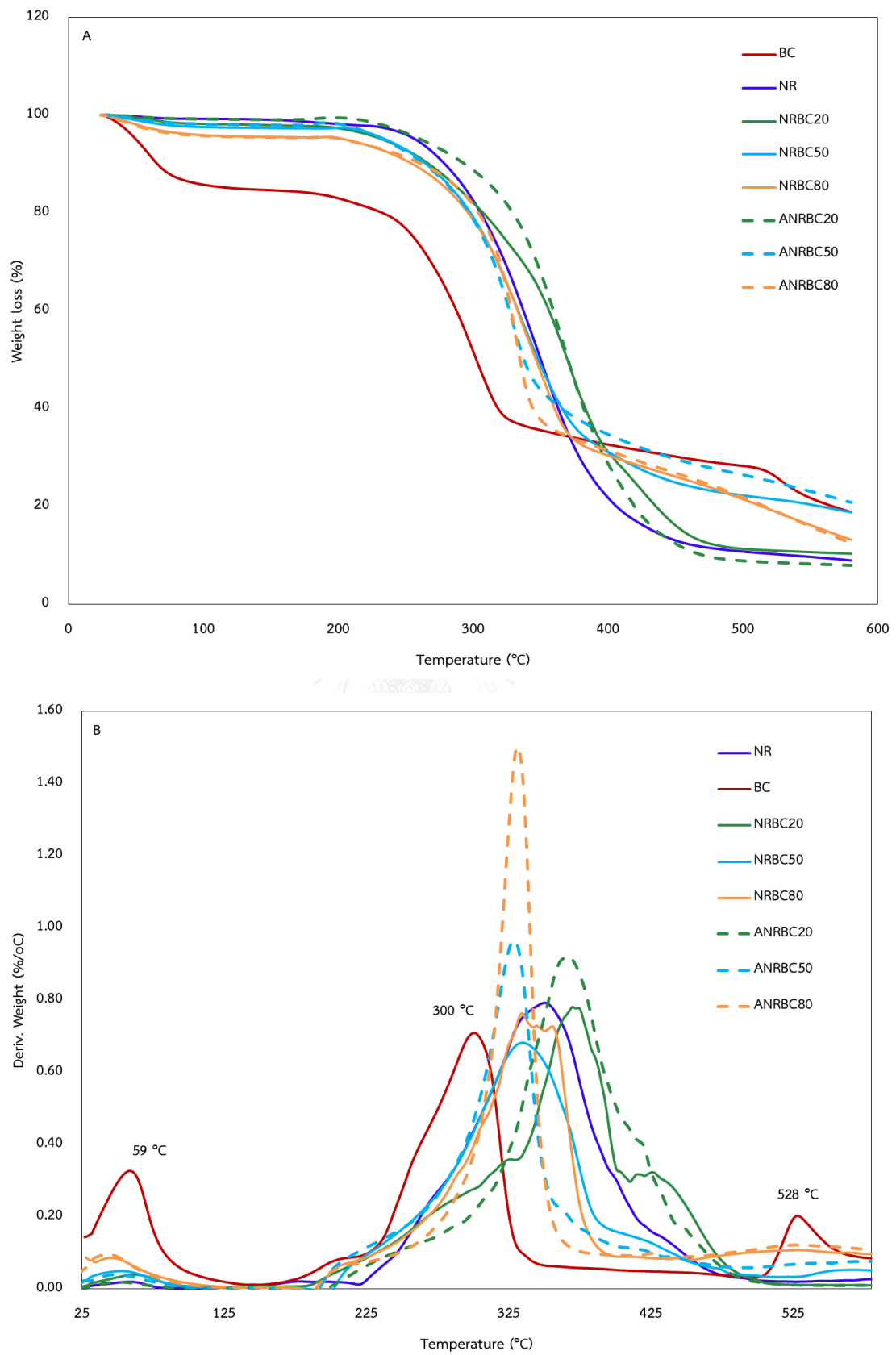


Figure 4.11 The TGA(A) and DTG(B) plot of NR, BC, NRBC, and ANRBC composites

4.2.7 Differential scanning calorimetry (DSC)

Fig.4.12A shows the DSC chromatograms of NR, BC, NRBC and ANRBC composites under second heating scan from -100 to 300°C to consult their T_g . Pure NR chromatograms appeared T_g at -63.6°C, whereas pure BC was not changed in the range -100 to 300°C. In case of the NRBC composites, their chromatograms appeared T_g at -63.4, -63.8 and -66.5°C for NRBC20, NRBC50 and NRBC80 respectively. Therefore, the reinforcement by adding BC fibers into NR matrix caused slightly changes of T_g . These could indicate the NR polymer mobility increase with the BC loading due to their porous or network structure. Thus, NRBC50 and NRBC80 had higher polymer flexibility or mobility than pure NR and NRBC20 [62, 63]. In case of the ANRBC composites, each films show the same T_g of NRBC composites that indicate the strong chemical bonding was not formed after the acid modification.

According to Fig.7B, DSC chromatograms under first heating scan from room temperature to 300°C of BC only show peak of T_m at 149.3 °C. There are the previous study that demonstrated T_g , T_c and T_m of BC at 22, 43 and 198 °C respectively [64]. The different T_g of BC that were measured is the result of the method of BC sample preparation such as BC crushing and cast-film process that had the effects on the structural arrangement. Due to T_m of pure NR is higher than BC, T_m of the composites decrease with the increasing of BC concentration. There is the previous study which reported the BC fibers can induce crystal nucleation at the fiber surface, i.e. the so-called transcrystallinity effect [65], and assist to rearrangement of molecular chain of NR. However, the decrease of T_m of the composites could be expected to be caused by the disorder or disarrangement of NR crystalline units as the BC fibers integrate into the NR matrix [66]. Moreover, the composites with high BC loading shown the low density materials due to the porous structure of BC fibers that is the cause of the accessible composite melting. In acid modified system, the ANRBC composites shown higher T_m and narrow peak of T_m when comparing with the NRBC composites. These are the evident of interfacial interaction between BC fibers and chain of NR and composite homogeneity. Formation of intra and inter molecular hydrogen bonds create the continuous BC fiber structure inside the NR matrix that enhances the

structural stability of the composites. In addition, there is the effect of the transcrystallinity that strongly reveals the nucleating role of the fibers, which are able to promote a more robust crystalline during the heating run. Beside the lactic molecules which were formed hydrogen bond with BC fibers lead to the increasing of composite density.

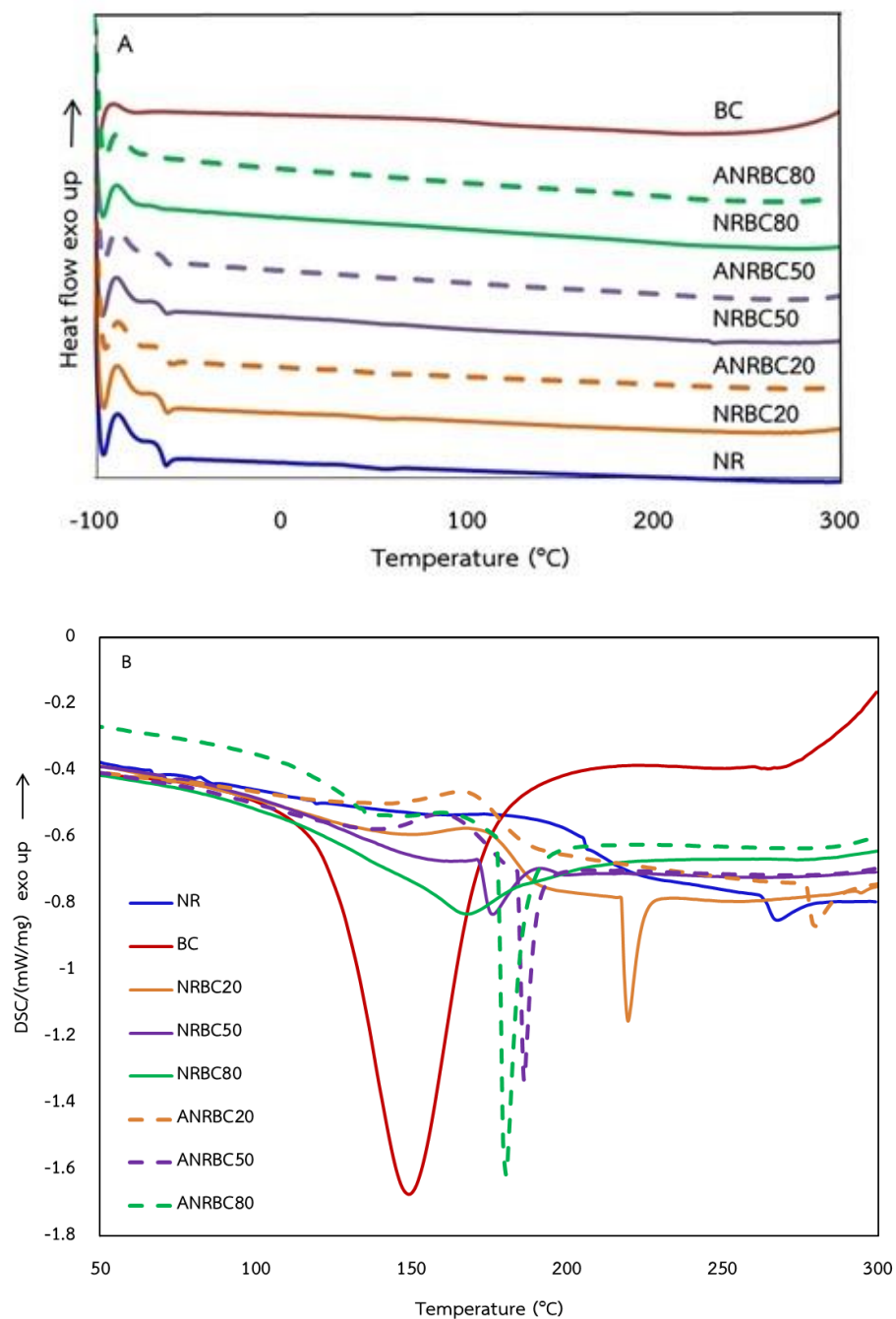


Figure 4.12 The DSC chromatograms of NR, BC, NRBC, and ANRBC composites

4.2.8 Dynamical mechanical thermal analysis (DMTA)

The dynamic mechanical properties of NR, BC, NRBC and ANRBC composites are studied over a wide temperature ranged from -100 to 40°C. The curves of storage tensile modulus (E') with the frequency at 1 Hz are displayed in Fig. 4.13A. The pure NR displays a typical behavior of amorphous polymers that their evolution of storage modulus corresponding to the typical for fully amorphous high molecular weight thermoplastic polymers [67]. On the other hand, BC curve displays a typical behavior of crystalline polymers. For the NRBC composites, the storage modulus in the glass transition region increases with BC loading, which implies an excellence reinforcement effect of BC fibers on NR. . The enhancement in below T_g is a good evidence for the strong reinforcing tendency of BC fibers in the NR matrix. A sufficiently strong interactions as well as the compatibility between NR and BC. Outstanding, NRBC20 has the highest dynamic mechanical properties in this temperature rang. This could be ascribed to NRBC20 is not only maintained the elastic properties of pure NR but also got the effects of the reinforcing with BC. However, the NRBC80 has the highest storage modulus in the rubbery region. The broad temperature range from -40 to 100°C of the rubbery plateau, resulting in a highly entangled state of the macromolecules, is ascribed to the polymers which have the high molecular weight. For the ANRBC composites, the lately interaction between BC and lactic acid has the effect on the mobility of rubber chains that are less flexible. Thus, it showed the less storage modulus in DMA curve. However, the ANRBC50 and ANRBC80 composites which were modified with lactic acid have the compatibility between the NR matrix and the BC fibers more than the NRBC composite. The interactions that occur after acid modification could reduce the polar of BC. The composite homogeneity was enhancing with the decreased of the difference of molecular polarity between the polymer matrix and the filler particle that were shown the narrow peak on the plot of $\tan \delta$ versus temperature (Fig.4.13B). Generally, the T_g of polymer can be shifted to higher temperature after incorporation of nanofillers. This is because nanofillers hinder the segmental motion of polymer chain segments [68]. However, No significant broadening of the $\tan \delta$ peak was observed except for the composites with 20 wt.% BC loading,

the T_g was improved by acid modification. This can be attributed 20 wt.% BC fibers were well dispersed and well distributed in NR matrix without the effects of the BC fiber disorder and agglomeration. These results in the NR-BC interfacial adhesion and the structural stability of the composites which were enhanced with the acid modification.

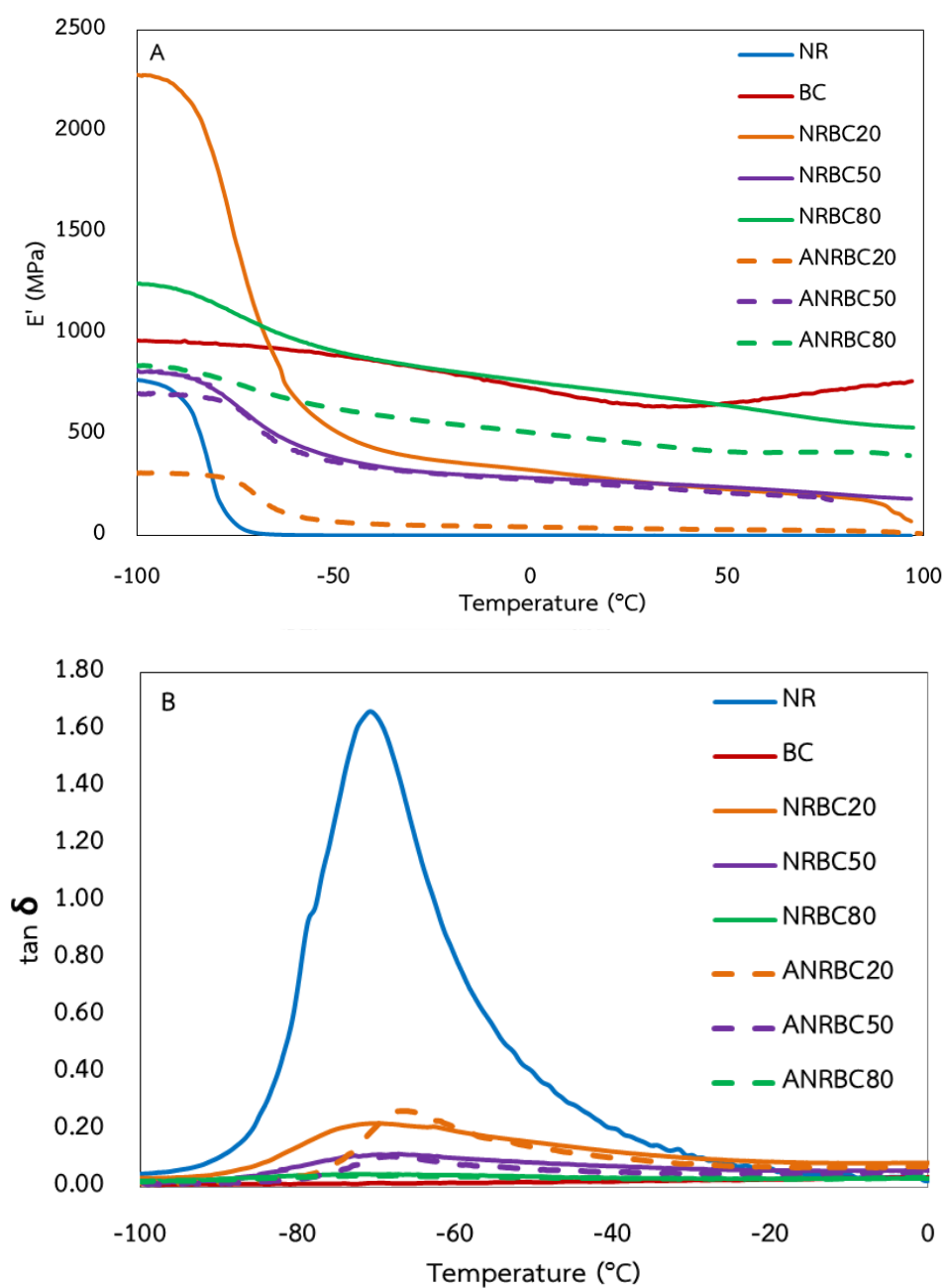
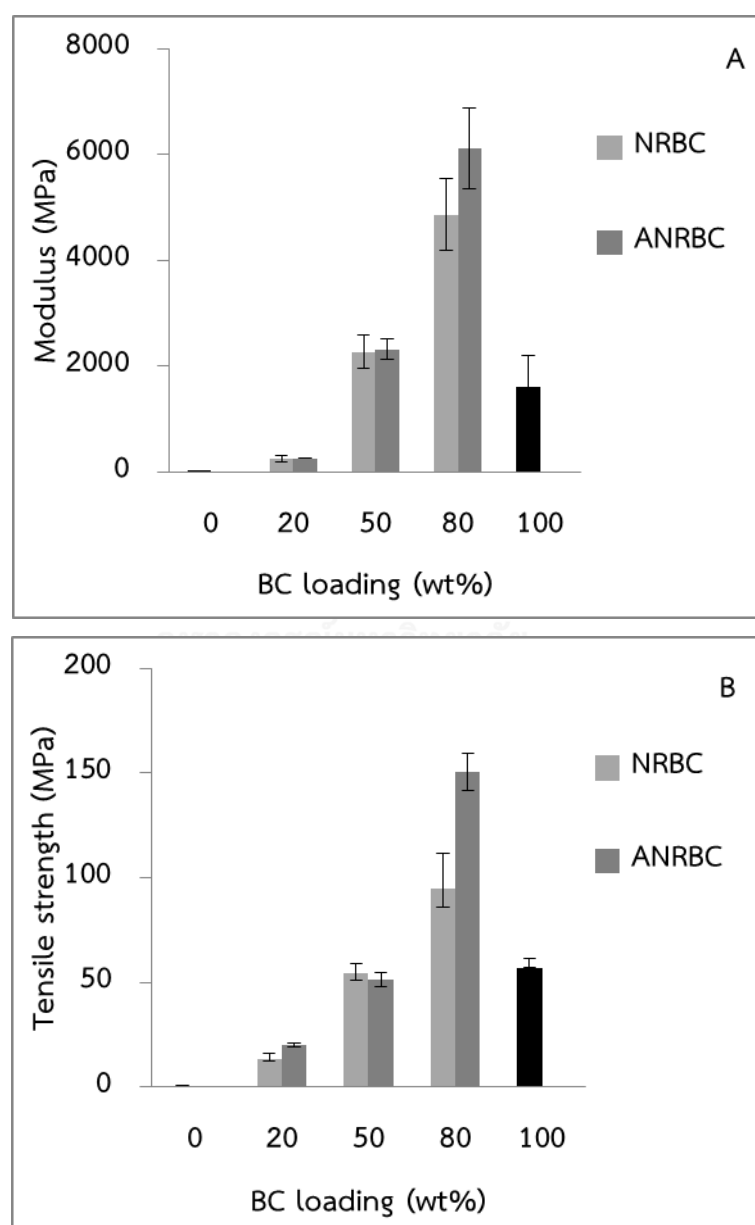


Figure 4.13 The temperature dependence of the storage modulus (A) and $\tan \delta$ (B) of NR, BC, NRBC and ANRBC composites

4.2.9 Tensile testing

The Young's modulus (Fig. 4.14A), tensile strength (Fig. 14.4B) and elongation at break (Fig. 14.4C) of NR, BC, NRBC and ANRBC dry films at different BC loading content were determined. In general, pure NR has low Young's modulus and tensile strength, but high elongation at break whereas BC has high Young's modulus and tensile strength, but low elongation at break. Overall, it was shown that BC fibers could be used as a reinforcing element in a NR matrix. Young's modulus and tensile strength of the NRBC films were enhanced with the increase of BC fiber contents. The maximal Young's modulus and tensile strength of NRBC composites at 4856.8 and 94.6 MPa, respectively were obtained with BC loading at 80%. OH groups create the inter and intra molecular interaction with hydrogen bonding. It was suggested that the NR chains might be immobilized by the network of BC fibers, which in turn increases the tensile strength and modulus of the composites [69]. Moreover, inter and intra molecular interaction of OH groups on BC fibers lead the composite to enhance the composite rigidity. Hence, high modulus and strength are advantages of reinforcing process which is controlled by fiber contents. However, there are limitations of reinforcement such as elasticity decline. The decrease of elongation at break of the composites was observed as BC loading content was increased. Besides NR-BC compatibility and BC fiber dispersion and distribution in the composites might be reduced at high BC loading content. The extent of mechanical reinforcement can be limited by filler aggregation or agglomeration during the composite preparation due to inter-particle interactions leading to the formation of weak points. This lack of intimate interfacial adhesion can induce several irregularly shaped voids inside the composite film. The NRBC20 had the highest elongation at break 15.4%, which was about 0.13 of pure NR. Generally, NR has a very high elasticity; however the preparation steps such as aging and drying could also make the materials become less elastic. Reinforcement with the smaller particle showed better mechanical properties than the large particle filled NR reinforcement [6]. For the acid modification, ANRBC80 has the strongly higher tensile strength than NRBC80. This is an evident of interaction that occurs between the OH group of BC fibers and lactic acid. The acid promote the inter and intra molecular structure of BC

fibers that can be used to increase rigidity of the composites, because the cellulose whiskers with hydrogen bond forming can reduce the brittleness of the composite backbone. The enhanced rigidity observed for composites can also be linked, at least partially, to the increased degree of crystallinity of the matrix that is following to the result of the XRD patterns [70]. While ANRBC20 has better elongation at break than NRBC20. This indicates lactic acid support the interfacial adhesion between BC fibers and NR matrix.



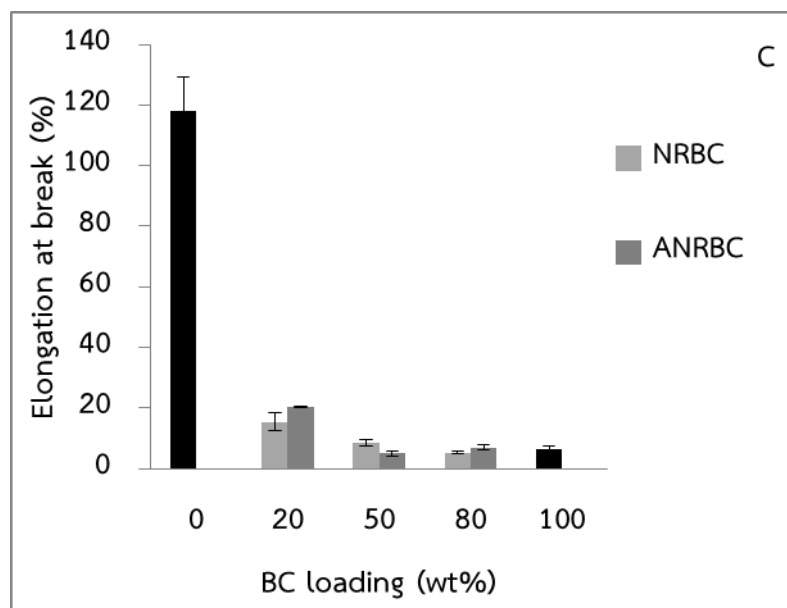


Figure 4.14 Mechanical test data of NR, BC, NRBC and ANRBC composites

The Young's modulus, tensile strength, and elongation at break determined from the stress-strain curves are shown in Fig.4.15. Elastic elongation is the most important characteristics of NR. Pure NR film has a high elastic elongation (118.2 ± 11.3 %). According to the stress-strain profile, the NRBC composites present considerably higher modulus and tensile strengths than NR. The modulus was increasingly enhanced with the rise of BC fiber contents, which should be due to the inclusion of rigid crystalline BC fiber into the rubber matrix. When crystalline cellulose was added into amorphous matrix of NR, crystallization of composite surface probably dominates over its bulk nature, giving higher modulus [69, 71, 72]. NR film is soft and tough. NRBC20 preserved the typical features of NR and were deficiently influenced by the presence of BC fibers, while NRBC80 were steadily influenced by the presence of BC fibers. Because of their high crystallinity, NRBC80 is hard and strong. For NRBC50, it is impartially between NRBC20 and NRBC80. For the ANRBC composites, there are slightly different behavior from NRBC composite. Due to the effects of hydrogen formation, ANRBC composites shown higher toughness than NRBC composites.

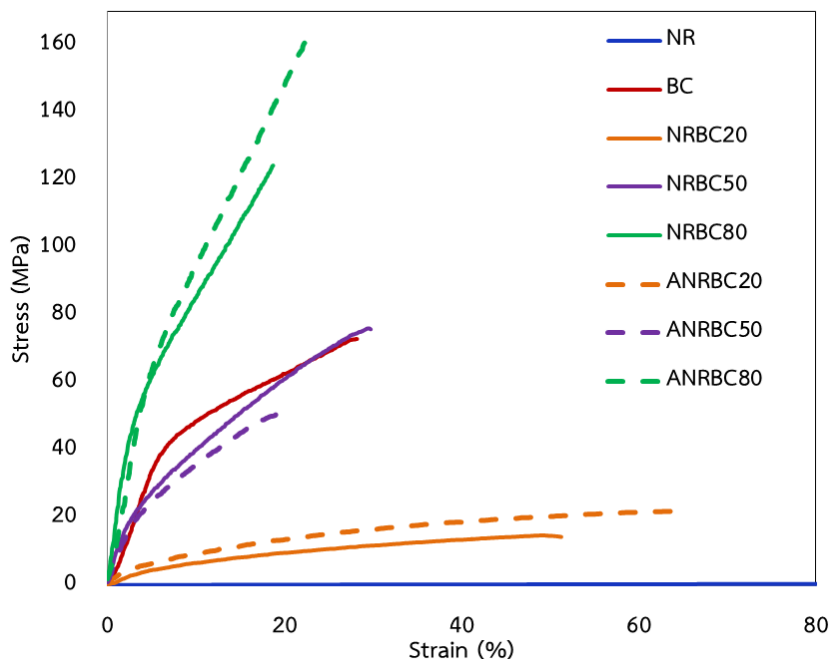


Figure 4. 15 The stress-strain curve of NR, BC, NRBC and ANRBC composites

4.2.10 The solvent uptake study

The degree of swelling of NR, BC, NRBC, and ANRBC composites at equilibrium are shown in Fig.4.16. The variation in solvent uptake by the composites with increase in BC loading is analyzed using toluene as the solvents (Fig.4.16A). Toluene is a solvent for the solubility of NR due to their similar values of the solubility parameters; $8.2 \text{ (cal/cm}^3)^{1/2}$ for NR and $8.9 \text{ (cal/cm}^3)^{1/2}$ for toluene[73]. Thus, NR could be dissolved and swelled in this non polar solvent. However, the degree of swelling decreases with the increasing of BC loading. This can be explained due to BC whiskers within the NR matrix which decreases the diffusion of the molecules of toluene into the NR matrix. It can also result from the strong interface between the BC fibers and the NR chains, constraining the swelling of the polymeric chains located in the interfacial zone [74, 75]. In addition, BC fibers also provides a tortuous path for toluene because of its polarity difference. The decrease in solvent uptake in composites can also be attributable in terms of the tortuosity of the path and the reduced transport area because of the decreased void formation with increased filler content in the composite membrane [35]. Furthermore, the ability of the composites to swell in toluene is also

due to the behavior of the filler itself. It was found that BC and most of its derivatives are insoluble in organic solvents [76]. In case of acid modification, ANRBC composites were swelled in toluene less than NRBC composites at 20 wt.% BC loading condition. This indicated the acid modification restrict the swelling of composites in the non-polar solvent. The hydrogen bond had the effect on the molecular information. Structure and molecular packing behavior of the composite with high molecular packing density are swelled less than the composites which loose molecular packing. Furthermore, hydrogen bond formation can be improved interfacial interactions that should restrict the diffusion of toluene molecules in the vicinity of the cellulosic surface. The inter and intra molecular structure of BC fibers which was promoted with lactic acid can enhances the structural stability of the composites. For the ANRBC50 and ANRBC80, there are no significant improvement. This is the result of the strongly difference of molecular polarity between BC fibers in the composites and toluene. Although there is the effects of acid modification, they present less than the effect of polar-nonpolar interaction.

In case of the degree of swelling of NR, BC, NRBC, and ANRBC composites in water as the polar solvent, they enhanced with the increasing of BC loading (Fig.4.16B). Due to the hydrophilicity of BC fibers, water were largely absorbed in the composites. This can be attributed to the increasing presence of OH groups. On the other hand, the hydrophilization of NR chains would of course increase their sensitivity to water [77]. Moreover the presence of natural fibers in the compound which increases the hydrophilic behavior of the composite, there is the effect of presence of filler particles in the matrix disturbing the structural homogeneity in the material, which can produce voids at the interface and may increase the ability of water molecules to penetrate the composite through capillary transport. It is expected that suitable compatibility between the phases should lead to a decrease [78]. For acid modification, there are the effects of the hydrogen bond formation like the toluene system. The strongly molecular packing or structural stability and improved interfacial interactions between the BC fiber and NR chains are also the factors of the decreasing of the degree of composite swelling. The improved interfacial interactions should inhibit the diffusion

of water molecules in the vicinity of the surface of BC fibers. However, there are significant development in the composites with 50% and 80% BC loading. This could be explained by the reducing of the composite hydrophilicity. Meanwhile, the hydrogen bond was formed by acid modification, the OH group on the BC structure was cover by the lactic molecules. In addition, a compatibility between amorphous phase and crystalline phase should decrease the total volume and size of voids in the composites that is the hindering of the water diffusion in the composites.

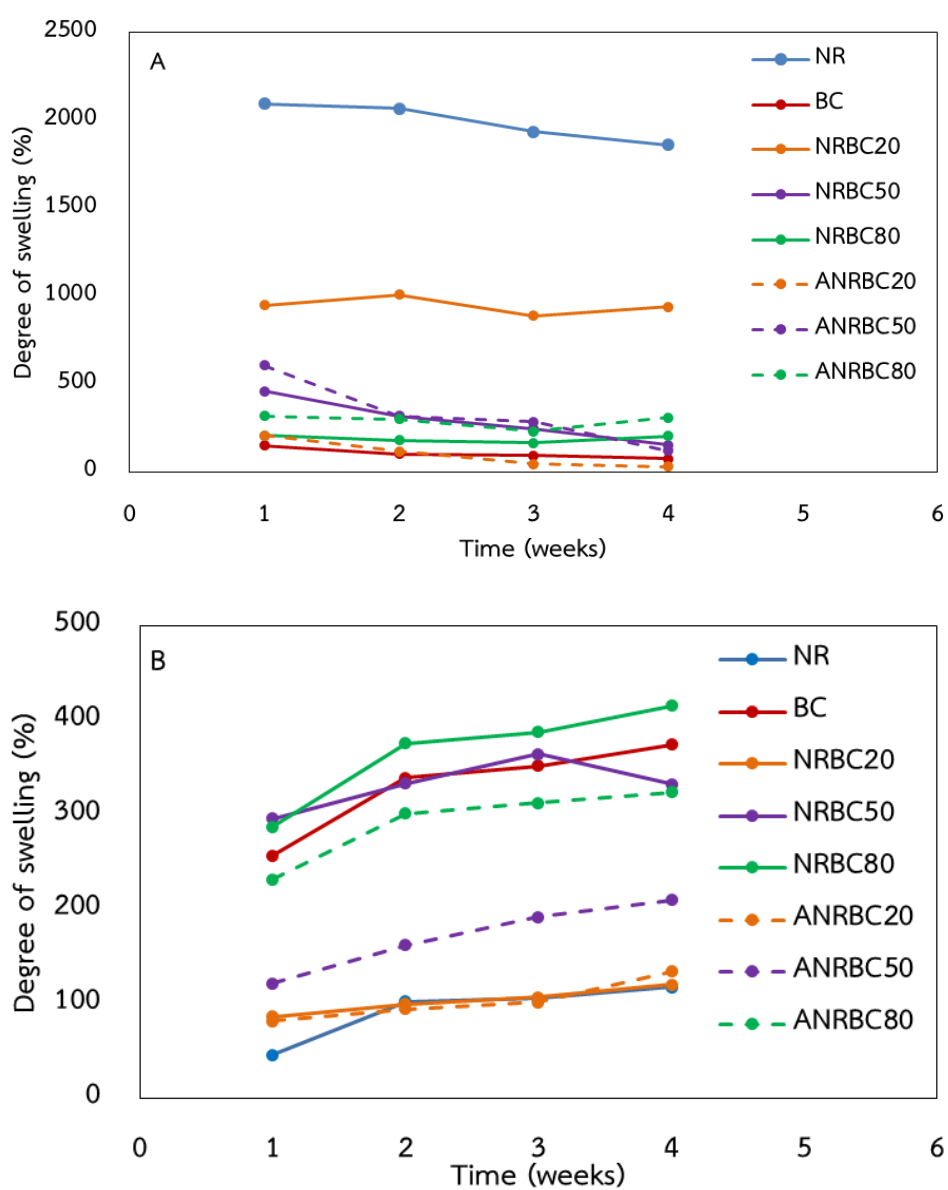


Figure 4.16 Degree of swelling of NR, BC, NRBC and ANRBC composites in toluene (A) and water (B)

4.2.11. The water vapor transmission rate (WVTR)

For food packaging applications, WVTR is the important properties that was determined because the bio-nanocomposite films must prevent moisture transfer between food and the surrounding atmosphere to be used [79]. Generally, the WVTR varies on some factors from the film dressing affected such as the viscosity of the film forming solution, the film formation procedure, and also film thickness [80, 81]. In this work, those factor had the effect on the WVTR when each condition with difference BC loading were compared. However, they could be neglect when comparing the WVTR between NRBC and ANRBC composites with equal BC loading. It is because there are no difference in the film forming solution, the film formation procedure, and also film thickness between the NRBC and ANRBC composites. According to Fig.4.17, the WVTR of NR is highest while BC shown the lowest. And the WVTR of the composites were enhanced with the increase of BC fiber contents. The improved WVTR could be according to the increase of degree swelling in water and hydrophilicity of the films. These were explained by the high hydrophilic nature of the whiskers in comparison with the pure NR matrix. This phenomenon exceeds the barrier property expected from them as the whiskers are thought to generate a more tortuous path for the vapor to travel across the composite thickness. Moreover, the crystallinity and the rod shape of the BC whiskers were related in mechanism of water transmission [67]. In case of the acid modification, there is the different between NRBC and ANRBC with 20 wt.% BC loading. It could be explained by the physicochemical characteristics of the acid modified surfaces and the effects of hydrogen bond information that leading to decreased porosity, void formation, and the loss of the integrity. The NR chains and BC whiskers were fixed with the hydrogen bond that seems to reduce the mobility of the polymer chains. Therefore, the molecules of water can transmits across the film less than the composites without acid modification. For 50% and 80% loading, there are no difference between NRBC and ANRBC. It indicated the effects of acid modification on the WVTR were weakly when compared with the effect of the hydrophilicity of the composites with high BC concentration.

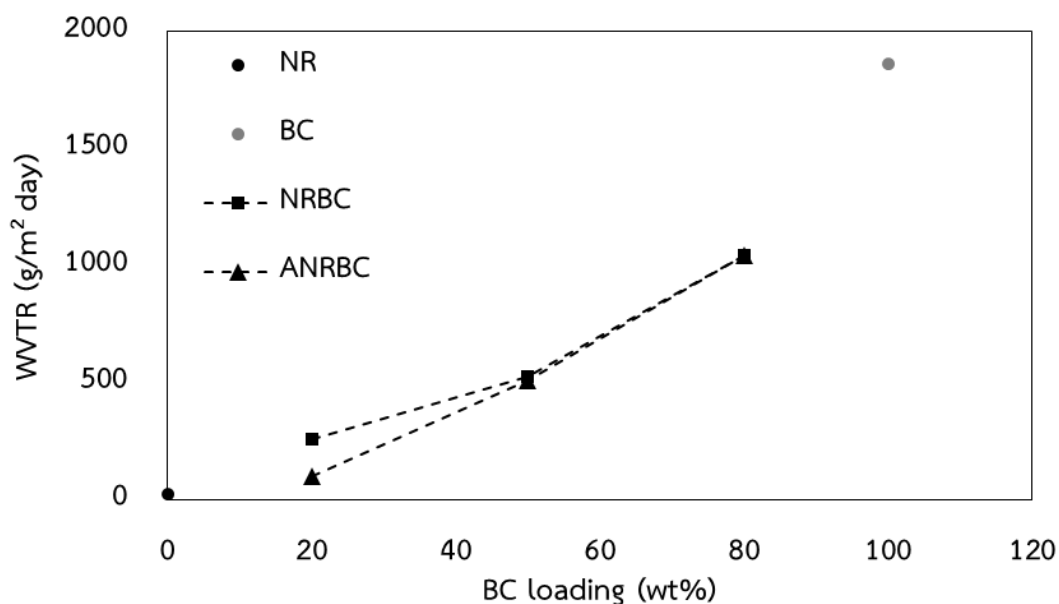


Figure 4.17 WVTR of NR, BC, NRBC and ANRBC composites

4.2.12 Biodegradation in soil

Biodegradable properties are important requirement in the area of packaging materials. Many studies have been carried out on the degradation of rubber [82]. NR degrades in nature by specific microorganisms in slow process and the growth of bacteria utilizing rubber as a sole carbon source is also slow [67]. Many bacterial strains that are able to utilize rubber as the sole source of carbon and energy, have been described [83]. These bacteria can be divided into two groups, which follow different strategies to degrade rubber [84]. Members of the first group form translucent halos if they are cultivated on solid media containing dispersed latex particles, indicating the excretion of rubber-cleaving enzymes. Members of the second group do not form halos and do not grow on latex plates; they require direct contact with the polymer. They grow adhesively at the surface of rubber particles in liquid culture, and they represent the most potent rubber-degrading bacterial strains [85]. In this work, there are uncontroled bacteria in soil. The experimental conditions were operated closely the environment as well as the humidity and temperature change with the variation of the weather. Daily weather reports of testing days (2015, August 26 – 2016, February 25) were referred in the appendix. According to Table 4.1, BC and the NRBC and ANRBC

composites with 80% BC loading were completely degraded in soil after being buried in soil for 3 months while pure NR lost about 5.95 % of its weight. Moreover, this table shows the presence of BC whiskers significantly enhanced biodegradation of rubber in soil. This is because cellulose biodegradation is faster than NR, cellulose component in the nanocomposites films is consumed by the microorganisms faster than rubber leading to increased porosity, void formation, and the loss of the integrity of the NR matrix. The rubber matrix will be broken down into smaller particles. Therefore overall faster disintegration of nanocomposites films containing cellulose whiskers than that of pure NR film is observed [67]. In case fo the acid modification, there is the significant effect on the composites with 50% BC loading. It could be explained by the hydrophilicity that ANRBC50 is swelling more than NRBC50 leading to increased porosity, void formation, and the loss of the integrity. Meanwhile, the insignificant effects of the acid modification were presented in the composites with 20% and 80% BC loading according to Fig.4.18. However, the acid modification for this study had almost no significant on its degradability in soil when compared with the NR/nanocellulose composites which were cross-linked in the potassium hydroxide solution. There are the significant effects on the this modification that the average degradation rate of the cross linked composites with 10% cellulose were approximately 0.15 times of the non-cross linked counterparts [86].

Table 4. 1 Weight loss of NR, BC, NRBC and ANRBC composites in soil

Sample	Weight loss (wt.%)		
	1 month	3 months	6 months
NR	4.08	5.95	5.83
BC	34.90	+++	+++
NRBC20	11.28	13.61	20.40
NRBC50	10.38	11.49	44.30
NRBC80	23.91	+++	+++
ANRBC20	9.62	12.84	15.17
ANRBC50	4.62	6.46	26.53
ANRBC80	53.28	+++	+++

(+++ : Completely degradation)

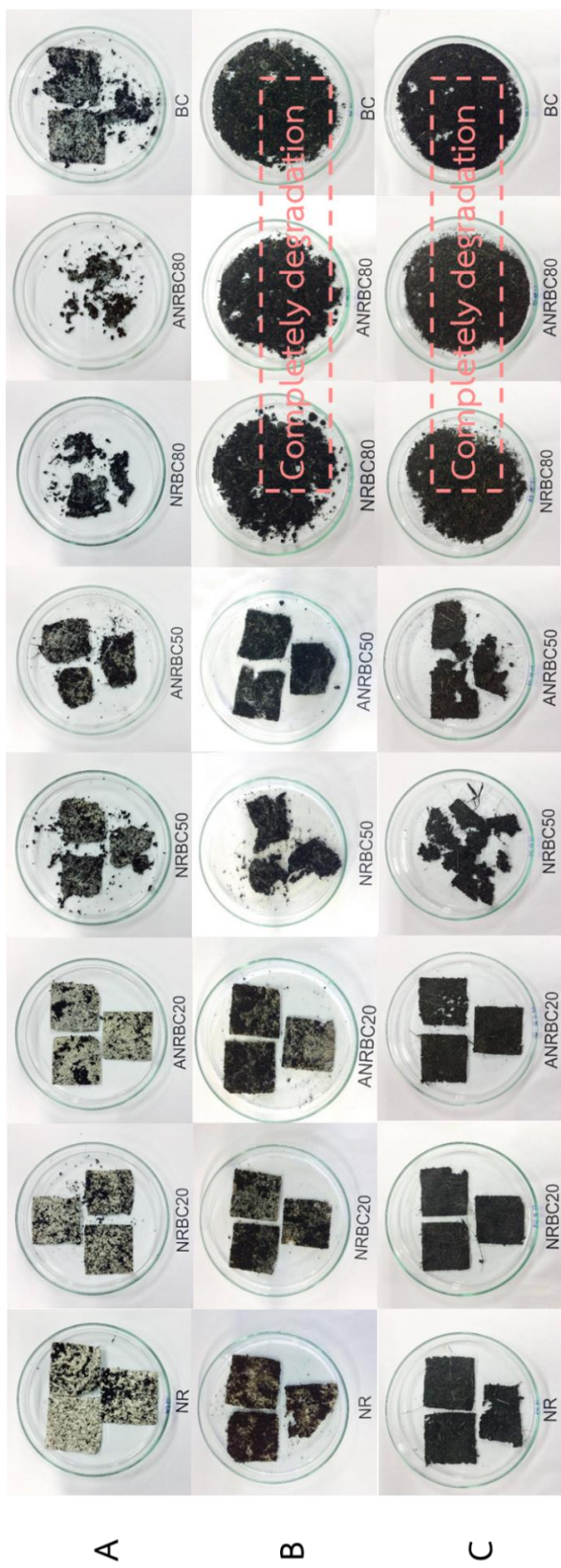
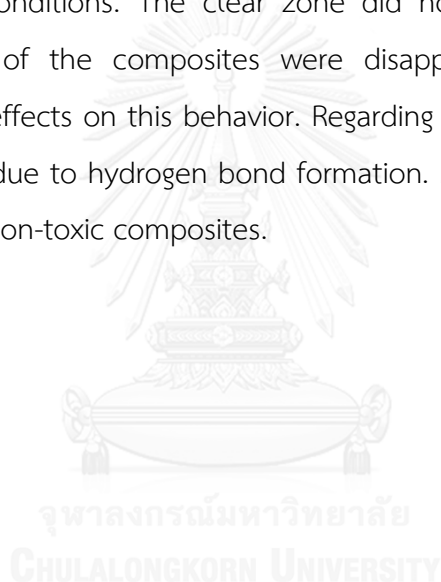


Figure 4.18 Biodegradation in soil of NR, BC, NRBC and ANRBC composites for 1(A), 3(B), and 6(C) months

4.2.13 Anti-microbial ability

Anti-microbial ability of the composites was studied, *E. coli* and *S. aureus* were used for the antibacterial tests. Each microbe was suspended in broth at the standardized concentration of 10^8 cells/mL prior to spreading 1 ml broth onto the agar plate. Sterilized neat NR films were employed as negative controls. Generally, the antibacterial activity was greater on *E. coli* than on *S. aureus* cells regardless of the times and temperatures [87]. For this study, the results revealed that the culture medium had no significant impact on the growth of *E. coli* (Fig.4.19A) and *S. aureus* (Fig.4.19B) in each conditions. The clear zone did not appear that indicates the antimicrobial ability of the composites were disappeared as well as the acid modification has no effects on this behavior. Regarding the ANRBC composites, lactic acid did not release due to hydrogen bond formation. Moreover, the disappeared of clear zone refer the non-toxic composites.



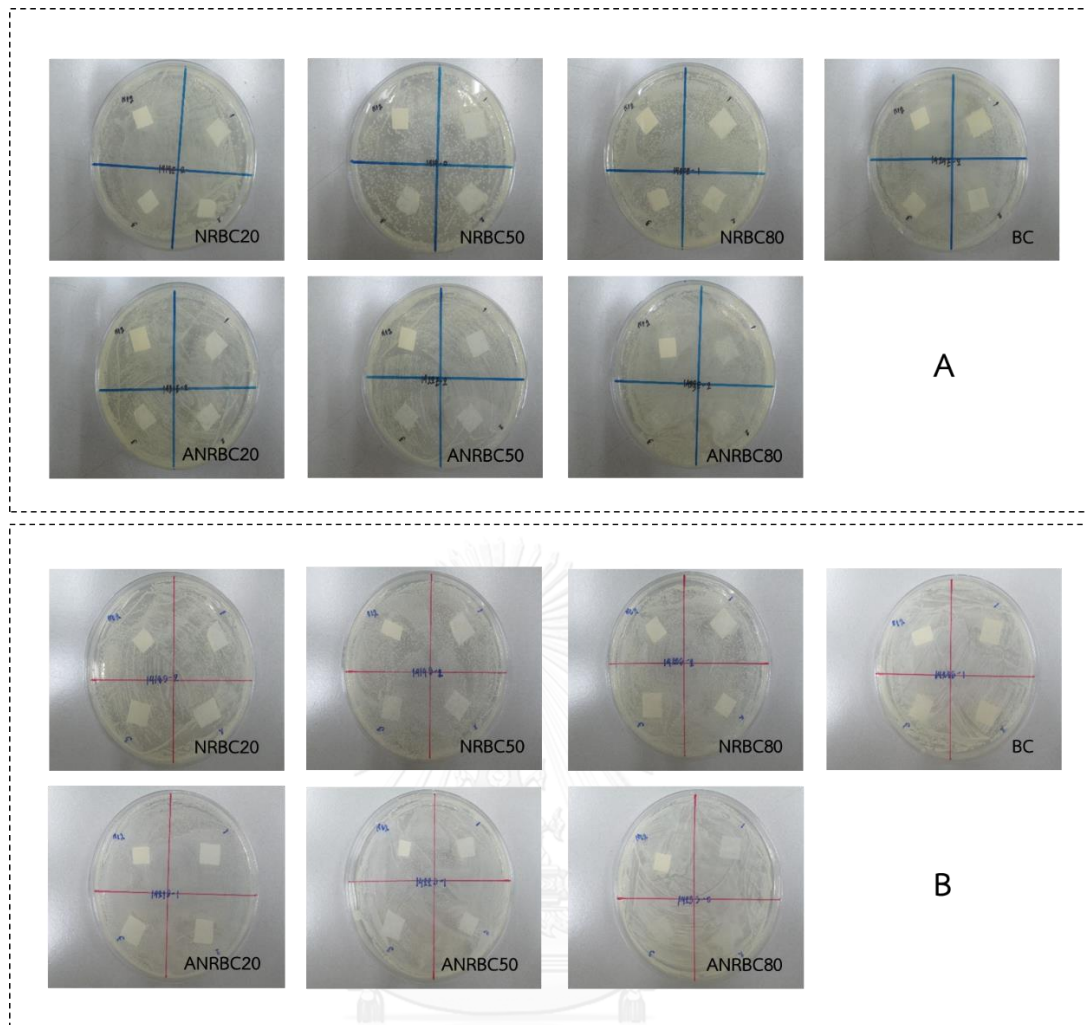


Figure 4.19 Antibacterial ability of NR, BC, NRBC and ANRBC composites

CHAPTER V

CONCLUSIONS

The NRBC composites were successfully prepared via latex solution process. BC fibers dispersed homogeneously within the NR matrix for every concentration with different BC fiber contents. Some weak interactions between BC fibrils and NR were illustrated. The hydrophilicity and crystallinity of the composite films increased when BC was added. The mechanical properties were effectively enhanced via reinforcement by BC fibers. NRBC80, which had highest Young's modulus and tensile strength of the NRBC composites, which were approximately 3707 times and 131 times, respectively of those of the NR films while NRBC20 composite film showed high elastic elongation and significant improvements in the Young's modulus and tensile strength with smooth surface. Additionally, an NRBC composite is more flexible in high BC fiber loading conditions at lower temperature. These highly mechanical performance composite material that shown a spectacular improvement of thermal stability are expected to find applications in rubber-based products and elastic packaging.

In addition, the interfacial interaction between NR and BC as well as the structural stability were improved by lactic acid modification. The hydrogen bond information lead to decreased porosity, void formation, and the loss of the composite integrity that are the limitation of the preparation of reinforced composite materials. ANRBC films shown the high performance more than NRBC films including mechanical properties, thermal stability, and chemical stability. However, by considering all composites, this improved interactions between NR and BC which were formed via the lactic acid modification had no significant effect on the biodegradability in soil. Thus, NRBC and ANRBC composites are suitable alternative materials for rubber-based products and elastic packaging during the environment friendly construction was strongly recognized.

REFERENCES

1. Rodgers, B., et al., *Rubber compounding*. 2004: Wiley Online Library.
2. Roberts, A.D., *Natural rubber science and technology*. 1988: Oxford University Press.
3. Leblanc, J.L., *Rubber–filler interactions and rheological properties in filled compounds*. *Progress in polymer science*, 2002. **27**(4): p. 627-687.
4. Ooi, Z.X., H. Ismail, and A.A. Bakar, *Optimisation of oil palm ash as reinforcement in natural rubber vulcanisation: A comparison between silica and carbon black fillers*. *Polymer testing*, 2013. **32**(4): p. 625-630.
5. Ikeda, Y. and S. Kohjiya, *In situ formed silica particles in rubber vulcanizate by the sol-gel method*. *Polymer*, 1997. **38**(17): p. 4417-4423.
6. Tangpasuthadol, V., et al., *Silica-reinforced natural rubber prepared by the sol-gel process of ethoxysilanes in rubber latex*. *Journal of applied polymer science*, 2008. **109**(1): p. 424-433.
7. Watcharakul, N., S. Poompradub, and P. Prasassarakich, *In situ silica reinforcement of methyl methacrylate grafted natural rubber by sol-gel process*. *Journal of sol-gel science and technology*, 2011. **58**(2): p. 407-418.
8. Cataldo, F., et al., *A comparative study on the reinforcing effect of aramide and PET short fibers in a natural rubber-based composite*. *Journal of Macromolecular Science, Part B*, 2009. **48**(6): p. 1241-1251.
9. Jayalatha, G. and S.K. Kuttu, *Effect of short nylon-6 fibres on natural rubber-toughened polystyrene*. *Materials & Design*, 2013. **43**: p. 291-298.
10. Raju, G., M.z.M. Said, and M.A. Ahmad, *Properties of Kenaf fibre reinforced natural rubber composites*. *JOURNAL OF RUBBER RESEARCH*, 2008. **11**(4): p. 187-195.
11. Anuar, H., et al., *Reinforced thermoplastic natural rubber hybrid composites with hibiscus cannabinus, l and short glass fiber—part i: Processing parameters and tensile properties*. *Journal of composite materials*, 2008. **42**(11): p. 1075-1087.

12. She, X., et al., *Molecular-level dispersion of graphene into epoxidized natural rubber: Morphology, interfacial interaction and mechanical reinforcement*. *Polymer*, 2014. **55**(26): p. 6803-6810.
13. Mohan, T., J. Kuriakose, and K. Kanny, *Effect of nanoclay reinforcement on structure, thermal and mechanical properties of natural rubber–styrene butadiene rubber (NR–SBR)*. *Journal of Industrial and Engineering Chemistry*, 2011. **17**(2): p. 264-270.
14. Valodkar, M. and S.I. Thakore, *Biopolymers as effective fillers in natural rubber: Composites versus biocomposites*. *Journal of Applied Polymer Science*, 2012. **124**(5): p. 3815-3820.
15. Zhou, Y., et al., *Lignocellulosic fibre mediated rubber composites: An overview*. *Composites Part B: Engineering*, 2015. **76**: p. 180-191.
16. Czaja, W.K., et al., *The future prospects of microbial cellulose in biomedical applications*. *Biomacromolecules*, 2007. **8**(1): p. 1-12.
17. Klemm, D., et al., *Bacterial synthesized cellulose—artificial blood vessels for microsurgery*. *Progress in Polymer Science*, 2001. **26**(9): p. 1561-1603.
18. Klemm, D., et al., *Cellulose: fascinating biopolymer and sustainable raw material*. *Angewandte Chemie International Edition*, 2005. **44**(22): p. 3358-3393.
19. Trovatti, E., et al., *Novel bacterial cellulose–acrylic resin nanocomposites*. *Composites Science and Technology*, 2010. **70**(7): p. 1148-1153.
20. Trovatti, E., et al., *Pullulan–nanofibrillated cellulose composite films with improved thermal and mechanical properties*. *Composites Science and Technology*, 2012. **72**(13): p. 1556-1561.
21. Trovatti, E., et al., *Simple green approach to reinforce natural rubber with bacterial cellulose nanofibers*. *Biomacromolecules*, 2013. **14**(8): p. 2667-2674.
22. McDonald, M.F., et al., *Polymerization processes*. 2007, Google Patents.
23. Kohjiya, S., et al., *Role of stearic acid in the strain-induced crystallization of crosslinked natural rubber and synthetic cis-1, 4-polyisoprene*. *Polymer*, 2007. **48**(13): p. 3801-3808.

24. Okwu, U. and F. Okieimen, *Properties of formic acid crosslinked epoxidized natural rubber (FC-ENR) blends with dry natural rubber*. European polymer journal, 1999. **35**(10): p. 1855-1859.
25. Pire, M., et al., *Imidazole-promoted acceleration of crosslinking in epoxidized natural rubber/dicarboxylic acid blends*. Polymer, 2011. **52**(23): p. 5243-5249.
26. Reddy, N. and Y. Yang, *Citric acid cross-linking of starch films*. Food Chemistry, 2010. **118**(3): p. 702-711.
27. Riyajan, S.-A., S. Chaiponban, and K. Tanbumrung, *Investigation of the preparation and physical properties of a novel semi-interpenetrating polymer network based on epoxised NR and PVA using maleic acid as the crosslinking agent*. Chemical Engineering Journal, 2009. **153**(1): p. 199-205.
28. Auras, R.A., et al., *Poly (lactic acid): synthesis, structures, properties, processing, and applications*. Vol. 10. 2011: John Wiley & Sons.
29. Kim, H., et al., *Graphene/polyethylene nanocomposites: effect of polyethylene functionalization and blending methods*. Polymer, 2011. **52**(8): p. 1837-1846.
30. Ismail, H., S. Salleh, and Z. Ahmad, *Properties of halloysite nanotubes-filled natural rubber prepared using different mixing methods*. Materials & Design, 2013. **50**: p. 790-797.
31. Soheilmoghaddam, M., M.U. Wahit, and N.I. Akos, *Regenerated cellulose/epoxidized natural rubber blend film*. Materials Letters, 2013. **111**: p. 221-224.
32. Tzounis, L., et al., *High performance natural rubber composites with a hierarchical reinforcement structure of carbon nanotube modified natural fibers*. Materials & Design, 2014. **58**: p. 1-11.
33. Jong, L., *Particle size and particle-particle interactions on tensile properties and reinforcement of corn flour particles in natural rubber*. European Polymer Journal, 2016. **74**: p. 136-147.
34. Qu, L., et al., *Remarkable reinforcement of natural rubber by deformation-induced crystallization in the presence of organophilic montmorillonite*. Acta Materialia, 2009. **57**(17): p. 5053-5060.

35. Abraham, E., et al., *Green nanocomposites of natural rubber/nanocellulose: membrane transport, rheological and thermal degradation characterisations*. Industrial Crops and Products, 2013. **51**: p. 415-424.
36. Rezende, C.A., et al., *Natural rubber-clay nanocomposites: mechanical and structural properties*. Polymer, 2010. **51**(16): p. 3644-3652.
37. Georjon, O. and J. Galy, *Effects of crosslink density on mechanical properties of high glass transition temperature polycyanurate networks*. Journal of applied polymer science, 1997. **65**(12): p. 2471-2479.
38. Visakh, P., et al., *Crosslinked natural rubber nanocomposites reinforced with cellulose whiskers isolated from bamboo waste: Processing and mechanical/thermal properties*. Composites Part A: Applied Science and Manufacturing, 2012. **43**(4): p. 735-741.
39. Chen, Y., D. Yuan, and C. Xu, *Dynamically vulcanized biobased polylactide/natural rubber blend material with continuous cross-linked rubber phase*. ACS applied materials & interfaces, 2014. **6**(6): p. 3811-3816.
40. López-Mata, M.A., et al., *Physicochemical, antimicrobial and antioxidant properties of chitosan films incorporated with carvacrol*. Molecules, 2013. **18**(11): p. 13735-13753.
41. Jokar, A., M.H. Azizi, and Z. Hamidi Esfehiani, *Effects of ultrasound time on the properties of polyvinyl alcohol-based nanocomposite films*. Nutrition and Food Sciences Research, 2015. **2**(4): p. 29-38.
42. Segal, L., et al., *An empirical method for estimating the degree of crystallinity of native cellulose using the X-ray diffractometer*. Textile Research Journal, 1959. **29**(10): p. 786-794.
43. Phisalaphong, M., T. Suwanmajo, and P. Sangtherapitikul, *Novel nanoporous membranes from regenerated bacterial cellulose*. Journal of applied polymer science, 2008. **107**(1): p. 292-299.
44. Iguchi, M., S. Yamanaka, and A. Budhiono, *Bacterial cellulose—a masterpiece of nature's arts*. Journal of Materials Science, 2000. **35**(2): p. 261-270.

45. Astley, O.M., et al., *Structure of Acetobacter cellulose composites in the hydrated state*. International journal of biological macromolecules, 2001. **29**(3): p. 193-202.
46. Raza, Z.A., et al., *Development of antibacterial cellulosic fabric via clean impregnation of silver nanoparticles*. Journal of Cleaner Production, 2015. **101**: p. 377-386.
47. Wei, L. and A.G. McDonald, *A Review on Grafting of Biofibers for Biocomposites*. Materials, 2016. **9**(4): p. 303.
48. Saurabh, C.K., et al., *Mechanical and barrier properties of guar gum based nano-composite films*. Carbohydrate polymers, 2015. **124**: p. 77-84.
49. Ye, Y., et al., *Macroscopic and Microscopic Analyses of Hydrophobic Modification of Rubbers with Silica Nanoparticles*. The Journal of Physical Chemistry C, 2015. **119**(36): p. 20957-20966.
50. Kirdponpattara, S., B.-M.Z. Newby, and M.K. Phisalaphong. *Effect of Oxygen Plasma Treatment on Bacterial Cellulose-Alginate Composite Sponge as a Yeast Cell Carrier for Ethanol Fermentation*. in *Advanced Materials Research*. 2013. Trans Tech Publ.
51. Phisalaphong, M., T. Suwanmajo, and P. Tammarate, *Synthesis and characterization of bacterial cellulose/alginate blend membranes*. Journal of Applied Polymer Science, 2008. **107**(5): p. 3419-3424.
52. Williams, D.B.G., et al., *Cellulose as a Source of Water Dispersible Renewable Film-Forming Materials*. Macromolecules, 2015. **48**(23): p. 8497-8508.
53. Hong, L., et al., *Hydroxyapatite/bacterial cellulose composites synthesized via a biomimetic route*. Materials Letters, 2006. **60**(13): p. 1710-1713.
54. Keshk, S. and K. Sameshima, *Influence of lignosulfonate on crystal structure and productivity of bacterial cellulose in a static culture*. Enzyme and Microbial Technology, 2006. **40**(1): p. 4-8.
55. Phisalaphong, M. and N. Jatupaiboon, *Biosynthesis and characterization of bacteria cellulose-chitosan film*. Carbohydrate Polymers, 2008. **74**(3): p. 482-488.

56. Chandra, J., N. George, and S.K. Narayanankutty, *Isolation and Characterization of Cellulose Nanofibrils From Arecanut Husk Fibre*. Carbohydrate Polymers, 2016.
57. Stading, M., A.-M. Hermansson, and P. Gatenholm, *Structure, mechanical and barrier properties of amylose and amylopectin films*. Carbohydrate Polymers, 1998. **36**(2): p. 217-224.
58. Ooi, Z.X., H. Ismail, and A.A. Bakar, *Study on the ageing characteristics of oil palm ash reinforced natural rubber composites by introducing a liquid epoxidized natural rubber coating technique*. Polymer Testing, 2014. **37**: p. 156-162.
59. Bendjaouahdou, C. and S. Bensaad, *The effects of organoclay on the morphology and balance properties of an immiscible Polypropylene/Natural Rubber blend*. Energy Procedia, 2013. **36**: p. 574-590.
60. Chirayil, C.J., et al., *Isolation and characterization of cellulose nanofibrils from Helicteres isora plant*. Industrial Crops and Products, 2014. **59**: p. 27-34.
61. Asaletha, R., M. Kumaran, and S. Thomas, *Thermal behaviour of natural rubber/polystyrene blends: thermogravimetric and differential scanning calorimetric analysis*. Polymer degradation and stability, 1998. **61**(3): p. 431-439.
62. Pichayakorn, W., et al., *Preparation of deproteinized natural rubber latex and properties of films formed by itself and several adhesive polymer blends*. Industrial & Engineering Chemistry Research, 2012. **51**(41): p. 13393-13404.
63. Honary, S. and H. Orafi, *The effect of different plasticizer molecular weights and concentrations on mechanical and thermomechanical properties of free films*. Drug development and industrial pharmacy, 2002. **28**(6): p. 711-715.
64. Iqbal, H.M., et al., *Laccase-assisted grafting of poly (3-hydroxybutyrate) onto the bacterial cellulose as backbone polymer: Development and characterisation*. Carbohydrate polymers, 2014. **113**: p. 131-137.
65. Sanchez-Garcia, M., E. Gimenez, and J. Lagaron, *Morphology and barrier properties of solvent cast composites of thermoplastic biopolymers and purified cellulose fibers*. Carbohydrate Polymers, 2008. **71**(2): p. 235-244.

66. Laborie, M.-P. and E. Brown, *Method of in situ bioproduction and composition of bacterial cellulose nanocomposites*. 2011, Google Patents.
67. Bras, J., et al., *Mechanical, barrier, and biodegradability properties of bagasse cellulose whiskers reinforced natural rubber nanocomposites*. *Industrial Crops and Products*, 2010. **32**(3): p. 627-633.
68. Cao, X., et al., *Preparation and properties of carboxylated styrene-butadiene rubber/cellulose nanocrystals composites*. *Carbohydrate polymers*, 2013. **92**(1): p. 69-76.
69. Thomas, M.G., et al., *Nanocelluloses from jute fibers and their nanocomposites with natural rubber: Preparation and characterization*. *International journal of biological macromolecules*, 2015. **81**: p. 768-777.
70. Siqueira, G., et al., *Thermal and mechanical properties of bio-nanocomposites reinforced by *Luffa cylindrica* cellulose nanocrystals*. *Carbohydrate polymers*, 2013. **91**(2): p. 711-717.
71. Ismail, H., M. Edyham, and B. Wirjosentono, *Bamboo fibre filled natural rubber composites: the effects of filler loading and bonding agent*. *Polymer testing*, 2002. **21**(2): p. 139-144.
72. Karmarkar, A., et al., *Mechanical properties of wood-fiber reinforced polypropylene composites: Effect of a novel compatibilizer with isocyanate functional group*. *Composites Part A: Applied Science and Manufacturing*, 2007. **38**(2): p. 227-233.
73. Grulke, E.A., E. Immergut, and J. Brandrup, *Polymer handbook*. 1999: John Wiley & Sons.
74. Gopalan Nair, K. and A. Dufresne, *Crab shell chitin whisker reinforced natural rubber nanocomposites. 1. Processing and swelling behavior*. *Biomacromolecules*, 2003. **4**(3): p. 657-665.
75. Raju, G. and M.R.H.M. Haris, *Preparation and characterization of acidified chitosan immobilized in epoxidized natural rubber*. *Polymer Testing*, 2016. **53**: p. 1-6.

76. Yoksan, R., et al., *Controlled hydrophobic/hydrophilic chitosan: colloidal phenomena and nanosphere formation*. Colloid and Polymer Science, 2004. **282**(4): p. 337-342.
77. Mariano, M., N. El Kissi, and A. Dufresne, *Cellulose nanocrystal reinforced oxidized natural rubber nanocomposites*. Carbohydrate polymers, 2016. **137**: p. 174-183.
78. Kakroodi, A.R., Y. Kazemi, and D. Rodrigue, *Mechanical, rheological, morphological and water absorption properties of maleated polyethylene/hemp composites: Effect of ground tire rubber addition*. Composites Part B: Engineering, 2013. **51**: p. 337-344.
79. Soni, B., M.W. Schilling, and B. Mahmoud, *Transparent bionanocomposite films based on chitosan and TEMPO-oxidized cellulose nanofibers with enhanced mechanical and barrier properties*. Carbohydrate Polymers, 2016.
80. Morillon, V., et al., *Factors affecting the moisture permeability of lipid-based edible films: a review*. Critical reviews in food science and nutrition, 2002. **42**(1): p. 67-89.
81. Phaechamud, T., P. Issarayungyuen, and W. Pichayakorn, *Gentamicin sulfate-loaded porous natural rubber films for wound dressing*. International journal of biological macromolecules, 2016. **85**: p. 634-644.
82. Bode, H.B., K. Kerkhoff, and D. Jendrossek, *Bacterial degradation of natural and synthetic rubber*. Biomacromolecules, 2001. **2**(1): p. 295-303.
83. Rose, K. and A. Steinbüchel, *Biodegradation of natural rubber and related compounds: recent insights into a hardly understood catabolic capability of microorganisms*. Applied and Environmental Microbiology, 2005. **71**(6): p. 2803-2812.
84. Linos, A., et al., *A Gram-negative bacterium, identified as Pseudomonas aeruginosa AL98, is a potent degrader of natural rubber and synthetic cis-1,4-polyisoprene*. FEMS Microbiology Letters, 2000. **182**(1): p. 155-161.
85. Shah, A.A., et al., *Biodegradation of natural and synthetic rubbers: a review*. International Biodeterioration & Biodegradation, 2013. **83**: p. 145-157.

86. Abraham, E., et al., *X-ray diffraction and biodegradation analysis of green composites of natural rubber/nanocellulose*. Polymer degradation and stability, 2012. **97**(11): p. 2378-2387.
87. Fortunati, E., et al., *Ternary PVA nanocomposites containing cellulose nanocrystals from different sources and silver particles: Part II*. Carbohydrate polymers, 2013. **97**(2): p. 837-848.





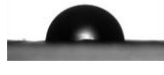

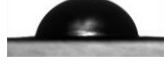
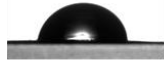


APPENDIX

Table 1 Data for Figure 4.6

Samples	Thickness (mm)	Opacity	
		Average	SD
NR	0.272	1.31	0.22
NRBC20	0.156	6.48	0.12
NRBC50	0.058	17.70	0.47
NRBC80	0.034	29.92	0.31
ANRBC20	0.19	4.71	0.16
ANRBC50	0.056	17.55	0.09
ANRBC80	0.03	33.10	0.28
BC	0.052	28.12	0.15

(SD: Standard deviation)

Table 2 Data for Figure 4.7

Samples	Contact angle		
	Average	SD	Image
NR	116.21	7.76	
NRBC20	105.63	2.01	
NRBC50	90.65	5.12	
NRBC80	88.32	5.48	
ANRBC20	88.70	7.08	
ANRBC50	93.73	4.95	
ANRBC80	81.25	4.36	
BC	47.47	2.77	

(SD: Standard deviation)

Table 3 Data for Figure 4.10

Samples	Degree of crystallinity (%)
NR	1.10
NRBC20	17.91
NRBC50	33.10
NRBC80	36.29
ANRBC20	19.58
ANRBC50	36.21
ANRBC80	50.60
BC	58.18

Table 4 Data for Figure 4.14

Samples	Modulus (MPa)		Tensile (MPa)		Elongation (%)	
	Average	SD	Average	SD	Average	SD
NR	1.31	0.09	0.72	0.02	0.09	11.25
NRBC20	249.05	60.79	13.55	2.76	60.79	2.96
NRBC50	2274.00	320.16	54.45	4.41	320.16	0.86
NRBC80	4856.75	675.72	94.63	17.31	675.72	0.27
ANRBC20	263.23	8.33	20.24	0.81	20.35	0.41
ANRBC50	2318.25	192.27	51.36	3.46	5.09	0.82
ANRBC80	6123.75	761.52	150.80	8.93	6.94	0.79
BC	1618.00	593.09	56.93	4.32	593.09	0.98

(SD: Standard deviation)

Table 5 Data for Figure 4.16A

Samples	Degree of swelling in toluene (%)			
	1 week	2 weeks	3 weeks	4 weeks
NR	2094.60	2066.89	1934.40	1858.83
NRBC20	946.2884	1007.66	887.234	938.7234
NRBC50	205.8531	116.9553	44.81138	28.48705
NRBC80	457.34	314.3036	244.1656	151.9448
ANRBC20	605.40	316.98	285.71	120.32
ANRBC50	205.89	180.66	164.09	202.58
ANRBC80	316.5644	299.3865	230.6748	307.9755
BC	148.14	101.95	92.91	73.43

Table 6 Data for Figure 4.16B

Samples	Degree of swelling in water (%)											
	1 week		2 weeks		3 weeks		4 weeks					
	Average	SD	Average	SD	Average	SD	Average	SD				
NR	46.08	14.06	102.49	44.08	105.75	35.86	117.76	27.12				
NRBC20	86.35	13.32	99.63	11.16	106.71	20.16	120.48	32.31				
NRBC50	295.72	20.97	333.30	43.20	364.09	64.64	332.24	66.24				
NRBC80	287.26	70.12	375.56	115.81	387.75	140.68	415.17	212.94				
ANRBC20	81.47	7.93	94.29	12.28	101.39	9.64	134.31	40.42				
ANRBC50	121.37	13.40	162.25	28.22	191.47	31.10	209.41	50.13				
ANRBC80	231.72	74.74	301.34	44.98	312.72	57.82	324.16	76.32				
BC	256.86	42.95	338.94	37.88	351.53	40.70	374.11	31.02				

(SD: Standard deviation)

Table 7 Data for Figure 4.17

Samples	WVTR (g/m ² day)
NR	24.8
NRBC20	258
NRBC50	524
NRBC80	1044
ANRBC20	101
ANRBC50	510
ANRBC80	1043
BC	1862

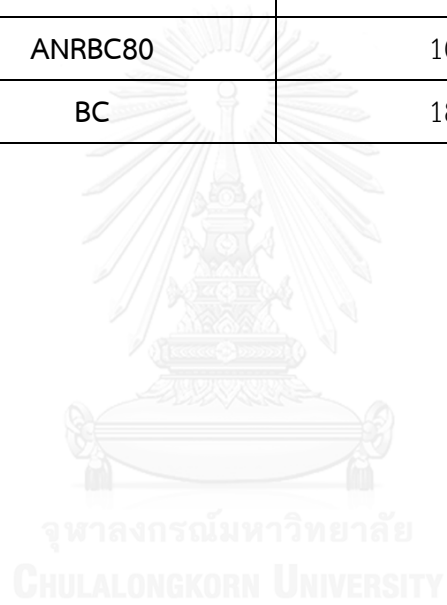


Table 8 Daily weather data for biodegradation testing

Date/ Month- Year	Average daily temperature (°C)						
	Aug-15	Sep-15	Oct-15	Nov-15	Dec-15	Jan-16	Feb-16
1	27.7	28.3	28.4	29	30.9	27.4	29.7
2	27.2	29.5	27.1	29.2	30.3	27.4	29.2
3	27.5	29.4	26.5	28.3	29.2	27.7	28
4	28.6	28.9	26.6	29	28.7	28.9	27.9
5	29.2	29.6	27.7	29.2	27.4	28.9	28.7
6	29.6	29.8	27.3	29.7	28.1	29	26.5
7	29.9	31	27.8	29	27.3	28.8	23.1
8	29.7	30.9	28.9	28.6	28.1	27.7	21.5
9	30.5	30.7	27.1	28.9	29	27.9	22.7
10	30.4	28	28	29.4	29	29	25.7
11	30.3	27.3	27.7	29.9	29.5	28.5	27
12	30	28.8	26.9	30.3	29.6	28.4	28.4
13	29.1	28.9	27.3	28.9	29.5	28.6	29.1
14	30.3	27.9	27.8	28.9	29.8	29.2	29
15	30.7	27.3	29.2	28.4	29.2	29.7	29.6
16	30.5	26.9	29.7	29	29.5	28.4	29.1
17	31	26.5	29.9	29.8	27.5	29.8	29.4
18	31.3	28.4	29.3	30.9	25.4	30.1	29.8
19	31.1	28.3	28.5	30.5	26.2	29.5	29.3
20	30.7	30.5	28.9	29.3	26.4	29.1	29.4
21	29.6	31.3	30.2	29.8	27.4	29.3	29.3
22	29.9	29.6	27.5	30.3	28.2	29.7	29
23	28.9	27.1	29.3	30.2	28.1	29.6	29.3
24	32.1	28.6	29.8	30.2	28.5	24.7	29.3
25	30.5	29.4	29.5	30.5	29.5	18.4	29.1

Table 8 Daily weather data for biodegradation testing (Continue)

Date/ Month- Year	Average daily temperature (°C)						
	Aug-15	Sep-15	Oct-15	Nov-15	Dec-15	Jan-16	Feb-16
26	29.9	30.3	29.7	30.2	29.9	19.8	29.5
27	29.3	29.9	29.1	29.3	29.6	21.3	28.9
28	28.3	28.8	29	28.9	29.4	24.9	28.8
29	29.4	27.9	29.2	29.7	29.2	28	29.3
30	30.4	28.7	30.6	30.2	29.2	28.9	-
31	29.7	-	30.3	-	28.5	29.5	-
Average	29.8	28.9	28.5	29.5	28.6	27.7	28.1



Table 9 Daily weather data for biodegradation testing

Date/ Month- Year	Relative humidity (%)						
	Aug-15	Sep-15	Oct-15	Nov-15	Dec-15	Jan-16	Feb-16
1	85	84	86	77	69	62	77
2	88	79	94	71	75	64	74
3	83	78	92	75	80	62	60
4	73	82	93	72	80	62	61
5	71	77	87	76	86	62	61
6	71	76	89	72	76	69	59
7	71	67	87	79	76	76	46
8	69	66	82	84	70	80	50
9	70	71	89	81	70	80	54
10	71	86	85	79	74	73	57
11	73	90	86	75	71	73	69
12	75	82	86	74	78	73	75
13	79	79	82	81	81	78	77
14	71	86	80	83	75	78	81
15	75	87	76	87	75	76	79
16	75	93	74	82	66	81	82
17	69	96	74	79	71	75	73
18	66	82	80	72	61	77	72
19	67	79	84	73	63	80	76
20	69	75	85	76	64	80	76
21	72	74	80	73	63	82	76
22	68	78	86	67	63	76	74
23	71	88	79	69	71	79	76
24	64	81	75	70	74	80	77
25	69	77	69	69	77	70	61

Table 9 Daily weather data for biodegradation testing (Continue)

Date/ Month- Year	Relative humidity (%)						
	Aug-15	Sep-15	Oct-15	Nov-15	Dec-15	Jan-16	Feb-16
26	69	74	68	71	75	64	51
27	76	78	77	65	74	72	54
28	84	85	78	67	65	68	54
29	73	87	79	69	63	69	56
30	71	85	71	70	63	78	-
31	74	-	72	-	62	79	-
Average	73	81	81	75	71	73	67



Table 10 Daily weather data for biodegradation testing

Date/ Month- Year	Rainfall (mL)						
	Aug-15	Sep-15	Oct-15	Nov-15	Dec-15	Jan-16	Feb-16
1	8.1	6.7	17.6	-	-	-	-
2	15.5	-	10.2	-	-	-	-
3	0.4	28.9	39.5	0.2	25.5	-	-
4	-	-	9.9	-	-	-	-
5	-	3.8	19	-	17.2	-	-
6	-	-	1.2	-	-	-	-
7	-	-	62.8	-	-	-	-
8	-	-	2.6	7.7	-	4.8	-
9	-	6.7	6.9	-	-	1.5	-
10	-	11.8	7.9	-	-	6	-
11	0.3	7	63.4	-	-	-	-
12	-	15	2.2	-	-	-	-
13	-	29.1	-	2.6	-	-	-
14	-	4	-	-	-	-	-
15	-	47.1	-	19.4	-	1.8	-
16	-	18.1	-	1	-	TRACE	-
17	-	20.5	-	-	-	-	-
18	-	36.2	1.7	-	-	-	-
19	-	-	0.2	-	-	32	-
20	-	-	3.8	0.3	-	5.1	-
21	2.2	0.2	-	-	-	0.3	-
22	-	2.8	48.3	-	-	-	-
23	-	17.1	-	-	-	2.7	-
24	-	T	-	-	-	18.4	-
25	-	2.2	-	3.7	-	-	-

Table 10 Daily weather data for biodegradation testing (Continue)

Date/ Month- Year	Rainfall (mL)						
	Aug-15	Sep-15	Oct-15	Nov-15	Dec-15	Jan-16	Feb-16
26	-	-	-	-	-	-	-
27	7.5	37.1	0.3	-	-	-	-
28	9.3	26.8	2.8	-	-	-	-
29	-	11.5	-	-	-	-	-
30	T	19.8	2.8	-	-	-	-
31	7.2	-	31.1	-	-	-	-
Total	50.5	352.4	334.2	34.9	42.7	72.6	-



VITA

Miss Sirilak Phomrak was born on October 16th, 1990 in Amnatcharoen, Thailand. She graduated with a Bachelor's degree of Science, majoring in Chemistry, Faculty of Science, Chulalongkorn University in 2012. In the same year, she started as a Master Degree student with a major in Chemical engineering, Faculty of Engineering and finished her study in December 2016.

Presentation in Conference:

March 2015: Oral presentation in 3rd International Conference on Polymers and Chemical Engineering (ICPCE'15). Bayview Hotel, Singapore

August 2016: Oral presentation in Advances in Functional Materials Conference 2016 (AFM-2016). International convention center (ICC), JeJu Island, South Korea